OULUN YLIOPISTO
UNIVERSITY of OULU

DEGREE PROGRAMME IN ELECTRICAL ENGINEERING

MASTER'S THESIS

MOBILE ANTENNA SOLUTION FOR THREE BAND DOWNLINK CARRIER AGGREGATION

Author	Juha-Matti Harju
Supervisor	Markus Berg
Second Examiner	Erkki Salonen
Technical advisor	Antti Karilainen

February 2014

Harju J. (2014). Mobile Antenna Solution for Three Band Downlink Carrier Aggregation. University of Oulu, Department of Communications Engineering, Degree Programme in Electrical Engineering. Master's Thesis, 73 p.

ABSTRACT

This thesis is a comparison of different mobile antenna solutions suitable for three band downlink carrier aggregation in long term evolution (LTE) systems. The most important comparable performance metric is the total efficiency including the required RF front end configuration. Also, the total volume occupied by the antenna elements and the transmission lines from the front end to the antennas is compared. Additionally, designed antennas should meet the set performance requirements antennas through specified frequencies for total efficiency, matching and envelope correlation coefficient of multiple input, multiple output (MIMO) antennas.

Two antenna configurations are presented in this thesis. The first presented model has separate antenna elements for all three bands using carrier aggregation. This solution is given with two different front end configurations. In the second solution, low and high frequency antennas are using a common antenna element.

The comparison of the designs is done by simulating the chosen structures implemented in a simple phone model with a time domain electromagnetic field simulator. Free space and hand grip situations are modeled and results are presented.

The results indicate that both proposals have similar total efficiencies. However, usage of separate antenna elements for all bands reduces the total antenna volume. Number of transmission lines needed in front end can be reduced from a total of six to four with a slight decrease in total efficiency to conserve space inside the device.

Key words: handset antenna, antenna volume, carrier aggregation

Harju J. (2014). Matkapuhelinantenniratkaisu kolmen kantoaallon yhdistämiseen. Oulun yliopisto, Tietoliikennetekniikan osasto, Sähkötekniikan koulutusohjelma. Diplomityö, 73 s.

TIIVISTELMÄ

Tässä työssä vertaillaan erilaisia kolmen kantoaallon yhdistämiseen soveltuvia matkapuhelinantenniratkaisuja LTE (long term evolution) -järjestelmissä. Työssä vertaillaan ensisijaisesti antennien sekä kunkin ratkaisun vaatiman RF-etuasteen kokonaishyötysuhdetta, antennien vaatimaa kokonaistilavuutta sekä ratkaisuihin liittyvien siirtolinjojen lukumäärää. Lisäksi toteutettujen antennien tulee täyttää asetetut vaatimukset kokonaishyötysuhteelle, sovitukselle ja MIMO (multiple input, multiple output) -antennien verhokäyrien korrelaatiolle.

Työssä esitellään kaksi erilaista antenniratkaisua. Ensimmäisessä ratkaisussa kaikille yhdisteltäville kantoaalloille varataan erilliset antennit. Tämä ratkaisu toteutetaan kahdella erilaisella etuasteella. Toisessa antenniratkaisussa alimmat ja ylimmät yhdisteltävät taajuudet käyttävät samaa antennielementtiä.

Toteutuksia verrataan simuloimalla yksinkertaiseen puhelinmalliin sijoitettuja antenniratkaisuja aikatasossa sähkömagneettisella kenttäsimulaattorilla. Vapaan tilan suorituskykyä on verrattu todelliseen käyttötilanteeseen simuloimalla esitetyt ratkaisut myös vasemman ja oikean käden otteissa.

Simulointien perusteella molempien antenniratkaisujen kokonaishyötysuhde on samaa luokkaa. Erillisiä antenneja käyttämällä saavutetaan kuitenkin sama kokonaishyötysuhde pienemmällä antennien kokonaistilavuudella. Tilan säästämiseksi RF-etuasteessa tarvittavien siirtolinjojen määrää voidaan vähentää kuudesta neljään pienellä kokonaishyötysuhteen heikennyksellä.

Avainsanat: matkapuhelinantenni, antennin tilavuus, kantoaaltojen yhdistely

TABLE OF CONTENTS

FOREWORD

Upon completion of this thesis, I would like to thank Nokia for offering an interesting topic with real need for my work. The work progressed much faster than expected when I started on it in November 2013. Still, despite the rather quick completion I feel that I have learned a lot from antennas and mobile telecommunications during the thesis.

I sincerely like to thank Dr. Antti Karilainen for guiding me through this task by giving good ideas and help always when needed. Also all other members of Nokia antenna technology team in Espoo deserve credit for the support throughout the time I have worked on this thesis.

I also appreciate the quick responses and feedback from both the supervisor Dr. Markus Berg and the second examiner Dr. Erkki Salonen from the university.

Last but not least, big thanks for my girlfriend, family and friends for support during this work and also during the seven years of studies in Oulu. Studies and everything else around them have been the best time of my life. However, now it seems that due to completion of this thesis, graduation threatens to put a halt to studies that started so well. Time to embrace something new!

Helsinki, February 10, 2014

Juha-Matti Harju

LIST OF ABBREVIATIONS AND SYMBOLS

3D	3-dimensional
3GPP	3rd Generation Partnership Project
CA	Carrier aggregation
CC	Component carrier
CST	Computer Simulation Technology
CTIA	The Wireless Association
ECC	Envelope correlation coefficient
EMC	Electromagnetic compatibility
ESR	Equivalent series resistance
FDD	Frequency division duplexing
FS	Free space
Gbps	Gigabits per second
HB	High band, frequency bands above 2.2 GHz
HL	Left hand grip
HR	Right hand grip
LB	Low band, frequency bands below 1 GHz
LTE	Long term evolution
MB	Mid band, frequency bands between 1.7 GHz and 2.2 GHz
MIMO	Multiple input, multiple output
MWS	Microwave Studio
PDA	Personal digital assistant
PIFA	Planar inverted F-antenna
Q	Quality factor
RX	Receiver
SAR	Specific absorption rate
SNR	Signal to noise ratio
SPxT	Single pole multi throw
TX	Transmitter
VSWR	Voltage standing wave ratio

λ	Wavelength
ρ_{in}	Reflection coefficient at matching circuit input
ρ_{L}	Reflection coefficient at antenna input
ρ_{out}	Reflection coefficient at matching circuit output
ρ_{P}	Power reflection coefficient
ρ_{S}	Reflection coefficient at source output
η_{m}	Matching efficiency
η_{mux}	Multiplexing efficiency
η_{rad}	Radiation efficiency
η_{tot}	Total efficiency

c	Speed of light in vacuum
$E_{\theta,\varphi X}$	Complex, polarized electric field pattern of antenna X
$E_{\theta,\varphi Y}$	Complex, polarized electric field pattern of antenna Y
ECC	Envelope correlation coefficient
f	Frequency
G_{T}	Transducer power gain
L	Inductance
L_{12}	Losses from generator to the load
L_{21}	Losses from the load to the generator
P_{θ}	Time average vertical power
P_{φ}	Time average horizontal power
P_{A}	Power available at the antenna terminals
P_{in}	Power fed to the input of matching network
Q	Quality factor
S_{ij}	Scattering parameter from port j to port i
R	Resistance
RL	Return loss
XPR	Cross polarization ratio
Z	Impedance
Z_0	Characteristic impedance of the transmission line
Z_{in}	Input impedance of antenna
Z_{R}	Reference impedance

1. INTRODUCTION

This work considers the design of antenna solution for mobile terminal using three band downlink carrier aggregation (CA) in long term evolution. In this scheme, one transmitter and three receivers are required to work simultaneously with additional three multiple input, multiple output receivers. This CA case has three downlink bands which are located in low band (LB) below 1 GHz, mid band (MB) around 2 GHz and high band (HB) above 2.3 GHz.

Target of the work is to simulate different antenna and front end structures with commercial electromagnetic simulation software manufactured by Computer Science Technology (CST) by using its time domain simulator. Based on simulation results total efficiency and total antenna volume of different solutions will be evaluated. Solutions compared for main antennas include design with separate antenna elements for all three bands and the design with common LB and HB antennas to go with separate MB element. Same design is also used for MIMO antennas.

Additional losses in RF front end caused by selecting some specific antenna solution are also inspected to some extent by including these losses to total efficiency comparison. Total losses depend on the solution specific number of required switches, diplexers and other components.

The key output of the thesis presents the comparison of the total efficiency and volume of two different antenna solutions suitable for three band downlink carrier aggregation cases.

Antenna is a device that transforms guided electromagnetic waves into radiated waves and vice versa [1]. Because radio link is the only transmission link in mobile devices, antenna performance is critical in enabling a link to the network and maintaining a good user experience at all times. However, handheld devices have multiple disadvantages from the antenna design point of view comparing to larger and more stationary devices.

First, frequencies used in global mobile telecommunications today range roughly from 700 MHz to 2.7 GHz. Even more frequencies for future use are expected but they are not yet widely used [2]. Generally lower frequencies attenuate less when propagating in free space which from the network operators' point of view encourages the usage of low frequencies. On the other hand, low frequencies are problematic in the mobile antenna design. To radiate efficiently at given frequency, the length of a traditional antenna should be at least near the quarter of its wavelength [3, 4]. Wavelength of an electromagnetic wave in free space is given as

$$\lambda = \frac{c}{f}, \tag{1}$$

where c is speed of light and f is the frequency of the electromagnetic wave [3]. Thus based on (1), wavelength in the mobile telecommunication frequencies in use varies between 0.11 m and 0.43 m. On the lowest used frequencies around 700 MHz

quarter of a wavelength is about 11 cm which is very close to the largest dimension of a modern day touch screen device. Major challenge in antenna design on low band frequencies below 1 GHz is to design well radiating antennas within such a small chassis. Later in this thesis overcoming this problem by using coupling elements to excite chassis radiation modes is discussed.

As said, laws of the physics demand antenna elements with certain size. On the other hand visual design and desire to create smaller and thinner devices demand antenna elements to be as small as possible [4]. Often handheld device antenna design is about balancing between sufficient performance and minimizing the antenna volume [4].

With current ramp up of LTE systems new important antenna related features are introduced to meet the increasing demand for higher data rates. For example, MIMO requires second separate receiving antenna. This of course adds pressure to reduce the size of a single antenna element. Carrier aggregation which is the main topic of this thesis is also new feature which affects the antenna design. In carrier aggregation, multiple carriers from different frequency bands are aggregated to increase the total bandwidth of a single user. Antenna related LTE features are discussed further in a separate chapter of this thesis.

User effect on small handheld device is also significant parameter. Portable devices are almost always used within the presence of a hand grip of the user. This may significantly decrease the performance of the antenna especially if not taken into account in the designing phase. [5]

2. ANTENNA PERFORMANCE QUANTITIES

2.1. Impedance matching

For sufficient power transmission between RF front end and antenna, impedances of antenna and the RF front end must be matched. Otherwise part of the propagating wave is reflected from the impedance discontinuity towards the source reducing the amount of the power transferred to the load. Voltage reflection coefficient at impedance discontinuity is given as

$$\rho_{\mathrm{L}} = \frac{Z_{\mathrm{in}} - Z_0}{Z_{\mathrm{in}} + Z_0}, \tag{2}$$

where Z_{in} is the input impedance of the antenna and Z_{o} is the characteristic impedance of the RF front-end transmission line [6, 7]. Magnitude of the reflection coefficient can be calculated also from known voltage standing wave ratio (VSWR) by using the formula

$$|\rho_{\mathrm{L}}| = \frac{VSWR-1}{VSWR+1}. \tag{3}$$

A logarithmic value of voltage reflection coefficient is called return loss. It can be obtained from [5]

$$RL = -20\log_{10}|\rho_{\mathrm{L}}|. \tag{4}$$

Matching efficiency, which can also be called transducer power gain G_{T}, illustrates the ratio between power available at the antenna terminals and power delivered to the matching network and it is calculated from

$$\eta_{\mathrm{m}} = G_{\mathrm{T}} = \frac{P_{\mathrm{A}}}{P_{\mathrm{in}}}, \tag{5}$$

where P_{in} is the total power available at the input of matching circuit and P_{A} is the power actually delivered to the antenna radiator [6, 8]. When voltage reflection coefficient at the matching circuit input is known, matching efficiency for lossless matching circuit can be calculated using formula [6, 7]

$$\eta_{\mathrm{m}} = (1 - |\rho_{\mathrm{in}}|^2). \tag{6}$$

Different reflection coefficients used in formulas (2) and (6) are visualized in Figure 1 which shows the source and the antenna impedances with 2-port matching circuit. In formula (6) the voltage reflection coefficient has the power of two as matching efficiency is used to describe behavior of the power. From formula (6) it can be seen that in ideal situation reflection coefficient would be zero to maximize the power transmission to antenna. However, it is important to note that maximum power transmission is achieved with voltage reflection coefficient being zero only if both

impedances in formula (2) are real. In general, maximum power transmission is achieved when impedances of formula (2) are complex conjugates which yield to non-zero voltage reflection coefficient. In this ideal case all available power would be delivered to the antenna from the source. However, perfect conjugate matching can be achieved only for a single frequency at a time in real situations. Thus it is necessary to accept certain level of mismatch to allow the design of broadband antennas [4, 9].

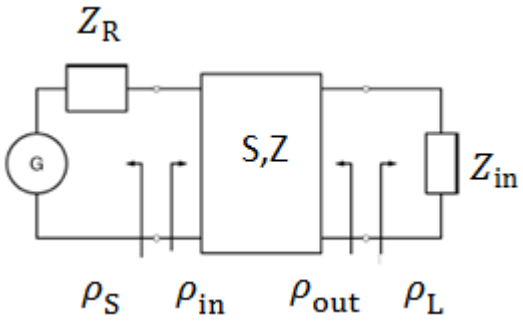

Figure 1. Reflection coefficients.

From formula (6) it can clearly be seen that in case of lossless matching components, minimizing the voltage reflection coefficient is a straightforward way to maximize the matching efficiency. In real situations matching components are lossy. In this case minimizing the reflections does not anymore guarantee high matching efficiency as in addition to mismatch losses also matching components cause losses. To better analyze lossy matching circuit performance, power wave definition of scattering parameters (S-parameters) is introduced. Traditionally, in microwave engineering S-parameters are defined by traveling waves which illustrate the behavior of voltage and current waves. On the other hand, in circuit simulation environments power waves are often used as they directly indicate the behavior of power. This is more convenient approach as the reflection coefficient of a power wave is zero when the maximal power transfer is achieved as opposed to nonzero voltage reflection coefficient of traditional traveling wave approach. Power wave reflection coefficient is given as

$$\rho_P = \frac{Z_{in} - Z_R^*}{Z_{in} + Z_R}, \tag{7}$$

where Z_R is the reference impedance. Based on formula (7), power reflection coefficient is zero when Z_R and Z_{in} are complex conjugates enabling maximum power transmission while reflection coefficient is zero. In this case, also the S-parameters S_{11} and S_{22} are zero. This simplicity is the key reason behind using power wave definition of S-parameters. [8, 9]

Power delivered from reference impedance Z_R shown in Figure 1 to antenna impedance Z_{in} is the transducer power gain which is simply

$$G_T = |S_{21}|^2. \quad (8)$$

Losses occurring in the matching circuit from the generator to the load can be calculated using

$$L_{12} = \frac{|S_{21}|^2}{1-|S_{11}|^2}. \quad (9)$$

Corresponding losses from the load to the generator can be calculated from

$$L_{21} = \frac{|S_{12}|^2}{1-|S_{22}|^2}. \quad (10)$$

In formulas (9) and (10) total losses through matching circuit, S_{12} and S_{21}, are assumed to be equal to retain the reciprocity of the circuit. Formulas (9) and (10) imply that losses in the matching circuit vary depending on the direction due to changing ratio between the losses from impedance mismatch and component non-idealities. If the impedance matching of the ports 1 and 2 differ much, it is expected that losses from non-ideal components are degrading the performance of the circuit. Losses from the matching components cause typically larger losses near the edges of the matching bandwidth which often leads to increased required impedance bandwidth to meet the efficiency requirements. Due to this, the best way to optimize matching circuit performance is to optimize the transducer power gain over required bandwidth instead of optimizing S_{11}. [8]

2.2. Antenna efficiency

Total efficiency of antenna η_{tot} denotes how big a portion of the power fed to the antenna matching circuit input is transformed to radiated power at the antenna [5]. For a single antenna it is defined as

$$\eta_{tot} = \eta_m \eta_{rad} = \frac{P_{rad}}{P_{in}}, \quad (11)$$

where η_{rad} is radiation efficiency of the antenna and P_{rad} is the power radiated from the antenna [6]. Total efficiency combines the effects of matching and radiation efficiencies.

In small sized device including multiple antenna elements, certain part of power radiated from one antenna element will be absorbed by other antenna elements(s). Same phenomenon occurs in receive mode as well, when a part of the arriving power is absorbed by the “wrong” antenna element. This effect is called mutual coupling and it is decreasing the efficiency of a single antenna radiating near other antenna(s).

Assuming that a single antenna is fed and other antennas are terminated to the characteristic impedance, the total efficiency of a single antenna in a multiantenna system can be expressed as

$$\eta_{\mathrm{tot},i} = \eta_{\mathrm{rad},i}\eta_{\mathrm{m},i}(1 - |S_{ii}|^2 - \sum_{i\neq j}|S_{ji}|^2), \quad (12)$$

where $\eta_{\mathrm{rad},i}$ is the radiation efficiency and S-parameters are related to antenna port i being fed. According to formula (12) mutual coupling to other antennas of the system S_{ij} reduces the total efficiency of an antenna. This yields to minimizing mutual coupling, in other words increasing isolation being an important design criterion. [10, 11]

2.3. Bandwidth of an antenna

Bandwidth of an antenna describes the frequency range where the antenna performance remains at an acceptable level for intended application [7]. In this thesis antenna matching, total efficiency and MIMO performance must fulfill the requirements through required bandwidth. Achievable bandwidth of antenna is affected by a few key factors. Antenna size was introduced earlier but especially in mobile devices the space reserved for antennas is often limited. Thus, antenna volume usually cannot be increased to gain bandwidth. Decreasing efficiency by using lossy matching components may be feasible in some applications but usually antenna efficiency requirements do not allow this. Also, reducing the dielectric constant of the substrate increases the bandwidth by increasing the effective length of the radiator. When size, efficiency and materials are locked, often the only way to improve the bandwidth of antenna is to use multiple resonances. Multiple resonances can be excited for example by using parasitic radiators or matching circuit with additional resonators. These extra resonators can be radiating themselves like parasitic radiators. However, usually additional resonators are non-radiating high-Q resonators like L-section matching resonators which still improve the bandwidth of the antenna. Advantage gained by increasing the number of matching resonances is limited to approximately three or four resonators. After that limit, performance approaches theoretical bandwidth limit defined by Bode-Fano –criterion [12, 13]. In this work design target is to use three or fewer matching resonators consisting of lumped elements. An L-shaped matching resonator can excite a single resonance and cascaded L-circuits can excite multiple resonances. [4, 14]

If sufficient bandwidth cannot be met with single matching circuit, also tunable matching circuits can be used to alter the matching between frequencies that are not required to operate simultaneously. Tuning circuits or tuners, for short, may consist of separate matching circuits selected by switches and/or tunable components like varactors. Tuning circuits allow also minimizing the antenna volume if bandwidth is otherwise sufficient. However, drawbacks of tuners include problems in linearity,

increased losses and complexity of design. In this thesis, simple tuners consisting of a single tunable capacitor or inductor are allowed. Tuning should be achieved by using a single pole, multi throw (SPxT) switch to select desired tuning component located parallel to the signal path. X in the abbreviation denotes the number of throws in the switch. For example SP2T switch has two throws. Non-idealities of switches cause additional losses in antenna matching circuit. However, in this thesis negative effects of tuners are not modeled. [4]

2.4. Radiation properties of an antenna

Radiation pattern describes 2- or 3-dimensionally what kind of spatial properties antenna radiation does have, usually in the far field. Radiation pattern can illustrate, for example, polarization, gain or phase. Mobile antenna design usually does not concentrate on radiation pattern optimization. This is due to fact that designer cannot do much to change the patterns, as especially on low frequencies the chassis is the main radiating element which causes radiation pattern to be very close to the pattern of half wave dipole despite orientation of antenna element. Similar but weaker phenomenon can be observed also in higher frequencies. Also patterns are bound to change when the user hand is brought near the device which would negate the possible benefits of radiation pattern optimization. [4, 5, 7]

Polarization is an antenna parameter which depends on the shape and orientation of the antenna. It is determined from the properties of a spherical wave transmitted from the antenna. Polarization of an antenna describes the behavior of electric field vector in the far field. In the far field plane of polarization is perpendicular to the propagation direction of a plane wave. Electric and magnetic field vectors are in this plane orthogonal to each other. Generally the tip of the electric field vector moves around the axis of propagation along elliptical path. The shape and orientation of this ellipse along with the rotation direction determine the polarization of a plane wave. [6, 7]

If polarizations of transmitting and receiving antenna are not matched, polarization mismatch loss is introduced [7].

Properties of the radiation pattern are not very important design criteria of mobile handset antennas. One of the key reasons behind this is mobile handset devices having an arbitrary orientation relative to incoming signal. Also, multipath nature of propagation environment causes some of the many arriving signal components to have same polarization as the antenna [4]. Normally antennas in mobile devices are considered to have a random elliptical polarization [4, 5]. However, different radiation patterns between main and MIMO antennas help to reduce envelope correlation coefficient (ECC) and thus improve MIMO performance. MIMO parameters are discussed deeper later in this thesis.

3. DESIGN ASPECTS FOR MOBILE TERMINALS

3.1. Antenna types used in this work

An antenna is considered electrically small if its longest dimension is shorter than one tenth of a wavelength in the operating frequencies of the antenna [3]. Traditional view usually regards internal handset antennas as self-resonant electrically small antennas which have very narrow bandwidths [5]. Despite self-resonant nature, it has been shown that the antenna element radiation is only 10% of total power at low frequencies while most of the radiation is contributed from the chassis unintentionally [15]. More recent approaches use small antenna elements as coupling elements to intentionally excite radiating modes in conductive chassis which is much longer comparing to wavelength, thus enabling wider bandwidths at low frequencies [16]. Frequencies used in this thesis have the maximum wavelength of 0.43 m at 699 MHz. The longest chassis dimension in the device used in this thesis is slightly over 120 mm which is more than one fourth of a longest used wavelength. So even though antenna elements themselves are small compared to wavelength, radiating system of chassis and antenna is considered “long” compared to wavelength. This means that antennas designed in this thesis are not electrically small.

Using coupling elements has several advantages over using electrically small antennas. Coupling elements do not need to be in resonance, so their size may be considerably smaller than self-resonant elements. This also makes design of the coupling elements simpler than for self-resonant antennas as no complex structures are needed to achieve resonance. However, coupling element may be also self-resonant on higher frequencies where it may be used as a traditional self-resonant antenna in addition to being a coupling element. Coupling elements are not frequency selective so very wideband solutions can be made by creating desired resonance for the combination of antenna and chassis with external matching circuit. This matching circuit may be tunable. [15, 16]

Coupling to chassis can be done by using either magnetic or electric fields. Ideal location and type for coupling element is totally different when using different fields to couple energy. In this thesis coupling is done via electric field. The level of coupling may be adjusted by tuning the shape, size and location of the antenna element which change the mutual capacitance between the antenna and the chassis. The best capacitive coupling is achieved when maximum of the electric field of the coupling element is co-located with the electric field maximum of the dominating chassis wavemode. Research has shown that the best positions for capacitive coupling element are in corners of the chassis and in shorter edge of the chassis. Optimal capacitive coupling element has such design that electric field is strong across the element. Because of this requirement, traditional planar inverted F–antenna (PIFA) is not optimal coupling element as near its shorting pin electric fields are weak. [15, 16]

Bandwidth of the combination of the chassis and the coupling element can be increased by improving the coupling between the coupling element and the chassis and reducing the unloaded quality factor of the antenna element. Coupling can be improved by increasing the volume and optimizing the positioning of the coupling element. [15]

3.2. Antenna locations in mobile terminals

Most mobile phones sold today are touch screen devices with body consisting of a single part. Device design prefers slim devices with screen covering as much as possible from the front surface. Due to metallic back of display panel acting as a ground plane, antenna placement is rather trivial – antenna must be located on the edges of the device. Side edges are not feasible locations as the device width beyond display should be minimized according to current trends. Additionally, the hand effect is obviously much larger on the sides compared to top and bottom parts of the phone. Limits on specific absorption rate (SAR) have been set by various organizations [5]. These regulations guide transmit antenna placement on the bottom part of the phone which is located farther from the user's head as opposed to location in top of the device where device is held against ear. Thus antennas to be used in transmission should be placed on the bottom of the phone. On the other hand, receive only antennas used for MIMO can be placed to top of the device where the effect of user hand is smaller than in bottom part of the device. However, MIMO antenna(s) can be placed on the bottom if there is enough space next to main antenna(s).

3.3. RF front end

RF front end consists of components and circuits between the transceiver module and the antenna. In mobile devices RF transceivers are heavily integrated circuits which have separate inputs and outputs for different cellular systems and frequency bands. Only filtering and multiplexing of signals is done outside the integrated circuit due to bulky components required for these tasks.

Separation of often closely spaced transmitter (TX) and receiver (RX) frequencies in frequency division duplexing systems (FDD) is achieved by using duplexers. Duplexers allow simultaneous traffic in uplink and downlink in same antenna by presenting sufficient isolation between RX and TX [1]. Loss estimate for a single duplexer used in this thesis is 2 dB.

A quadplexer combines the functionality of two parallel duplexers. These components have larger losses than duplexers, 2.5 dB is used in this thesis. These components are needed if two frequency bands connected to same antenna must be active at the same time which may be the situation with some carrier aggregation

cases. If needed, quadplexer is used to replace two parallel duplexers to prevent duplexers from loading each other.

The selection of the used duplexer or quadplexer and thus the frequency band is done by using switches which connect the antenna to the currently used line in RF engine. Switches introduce additional losses to the circuit. In this thesis this loss is considered to be 0.2 dB.

Diplexer is a component or circuit with three ports which can be used to multiplex signals in frequency domain to allow simultaneous use of transceivers using different frequency ranges [1]. They can be used to separate frequencies far enough from each other. In the scope of this thesis, diplexers can be used to separate LB from MB or HB. However it cannot be used to separate MB from HB as the bands 1 and 30 defined by 3rd Generation Partnership Project (3GPP) have very narrow separation, only 135 MHz. Typical loss for a single diplexer in circuit is around 0.4 dB through the cellular frequencies which is used in estimation of total efficiency in this thesis.

Depending on the antenna configuration type of the required components and thus also the losses in the RF front end vary. This is an important factor and must be kept in mind when designing antennas as increased antenna efficiency may be negated with complex RF front end. In scope of this thesis this is even more important as carrier aggregation sets more requirements for RF front end. These requirements are introduced later.

Transmission lines are used to deliver the signals from the RF front end to the antennas. Transmission lines consume lot of space, so the number of transmission lines should be as low as possible to save space inside the device. The number of required transmission lines is determined mainly by RF front end configuration. However, also the location of the front end has some effect on the number of transmission lines. For example, if the front end is near the main antenna, antennas can be fed on PCB without space consuming transmission lines like coaxial cables.

In Figure 2 simplified block diagram of a front end with s single antenna is shown to illustrate typical components and their functions. Antenna switch is used to select which duplexer is operational and connected to antenna. Traditionally only a single duplexer is connected to the antenna at a time. However, carrier aggregation changes also this as multiple bands (duplexers) are needed to match simultaneously which is a bit problematic. Later on solving this issue is discussed and front end configurations suitable for CA operation are shown.

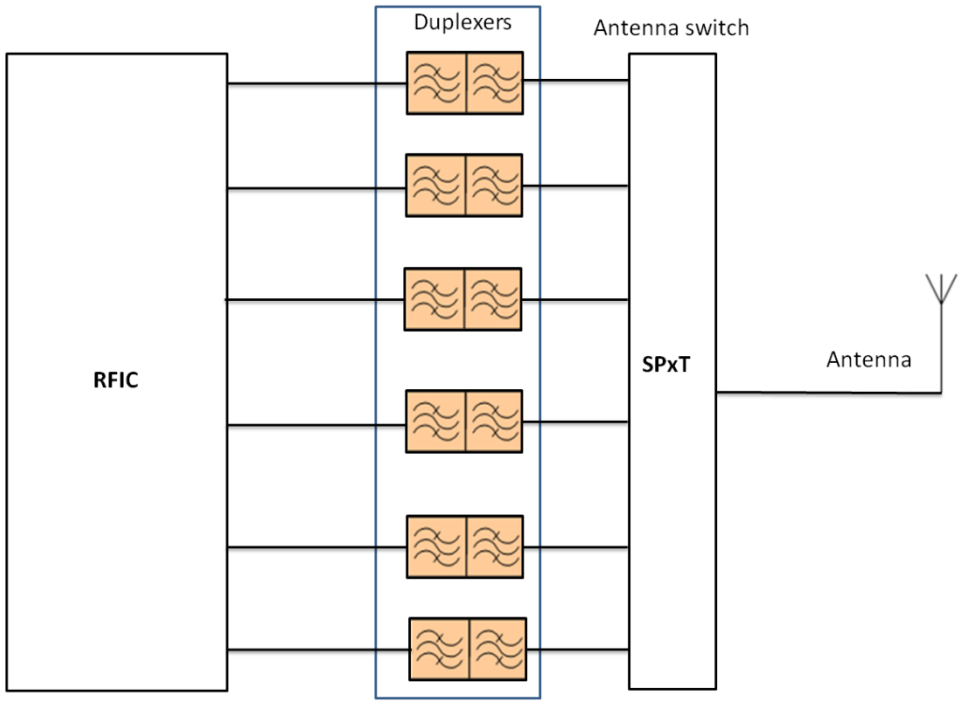

Figure 2. Simplified block diagram of a front end with a single antenna. Separate RX/TX connections between RFIC and duplexers are not shown.

4. ANTENNA RELATED FEATURES ENHANCING DATA RATES IN LTE

4.1. Multiple Input, Multiple Output

In LTE systems multiple input, multiple output systems are introduced. Using MIMO allows the usage of multiple transmitter and receiver antennas to reduce the effects of fading by diversity or to improve data rates by using parallel data streams. When MIMO is used in a channel with low signal to noise ratio (SNR), it is used to gain diversity. This means same data stream is received in multiple antennas simultaneously and received signals are combined to improve SNR and thus the reliability of the link. When SNR is high, MIMO is used in spatial multiplexing mode which utilizes different data streams using the same frequency between transmitting and receiving antenna pairs. Separate channels are separated spatially and thus do not interfere in ideal case. This enables higher data rates with no need for additional spectrum. In this chapter few performance metrics of MIMO antennas are introduced. [10, 18]

Envelope correlation coefficient is a parameter describing the independence of signals received by two antennas. ECC takes into account amplitude, phase and polarization properties of the radiation patterns of the two antennas and its approximation can be calculated from

$$ECC = \left(\frac{\oint \left(XPR \cdot E_{\theta X} E_{\theta Y}^{*} P_{\theta} + E_{\varphi X} E_{\varphi Y}^{*} P_{\varphi} \right) d\Omega}{\sqrt{\oint \left(XPR \cdot E_{\theta X} E_{\theta X}^{*} P_{\theta} + E_{\varphi X} E_{\varphi X}^{*} P_{\varphi} \right) d\Omega \oint \left(XPR \cdot E_{\theta Y} E_{\theta Y}^{*} P_{\theta} + E_{\varphi Y} E_{\varphi Y}^{*} P_{\varphi} \right) d\Omega}} \right)^{2}, \quad (13)$$

where $E_{\theta,\varphi X}$ and $E_{\theta,\varphi Y}$ are the complex polarized electric field patterns of two separate antennas X and Y. In (13) P_{θ} is the time average vertical power, P_{φ} corresponding horizontal power and cross polarization ratio XPR is the ratio between P_{θ} and P_{φ}. [10, 18]

Maximum theoretical envelope correlation coefficient between two antennas is equal to unity when antennas have identical radiation patterns and same location. When designing MIMO antennas, ECC should be as low as possible to achieve better MIMO performance. This is clear as in diversity mode uncorrelated radiation patterns of receiving antennas pick up signals from different directions and polarizations which reduces the probability of both signal paths fading simultaneously and thus allows good reception even with one path fading. In mobile phones, a rough design target for low band ECC is less than 0.5 and for mid and high bands less than 0.2 [10]. Low frequencies are usually problematic as the chassis of mobile device radiates 90% of the power in those frequencies which yields inherently more correlating antennas as all MIMO antennas are partially using same radiator and resonance mode of the ground plane [15].

Branch power difference denotes the difference of total efficiencies of two parallel MIMO paths. If the branch power is not equal, the capacity of the parallel spatial channels is reduced. Also diversity performance suffers from gain imbalance. Due to this, it is crucial to design MIMO antennas with efficiency almost equal to main antenna efficiency. [17]

A concept of multiplexing efficiency has been introduced. It is a useful parameter for antenna engineers designing MIMO antennas because it combines ECC and branch power difference to one single metric. It gives a simple decibel value to describe the relative efficiency loss of designed MIMO antennas comparing to ideal non-correlating antennas with equal efficiencies. When envelope correlation coefficient *ECC* and individual efficiencies η_1 and η_2 of two antennas are known, multiplexing efficiency is

$$\eta_{\text{mux}} = \sqrt{\eta_1\eta_2(1 - |ECC|^2)}. \tag{14}$$

Shown formula (14) is an approximate assuming high SNR levels. [19]

The design of MIMO antennas is done by following aforementioned guidelines. Usually when antennas are used on MB and HB, by reducing the mutual coupling sufficiently good ECC and efficiency can be achieved. On LB frequencies where chassis acts as a radiator reducing mutual coupling is not anymore important. Instead reducing ECC and improving efficiency should be straightforward targets. Performance of the designed MIMO solution should be verified also in the presence of the user hand and head.

4.2. Carrier Aggregation

Due to ever-increasing need for higher data rates, carrier aggregation is introduced in LTE-Advanced (LTE-A). It helps fulfilling the need to increase the data rates by increasing the usable bandwidth. The basic idea is to combine multiple carriers as opposed to usage of single carrier in earlier releases. LTE without CA can use a single carrier with different bandwidths the maximum being 20 MHz. With CA in LTE-A multiple carriers can be given for a single user to achieve faster data rates. In future releases maximum aggregated bandwidth of 100 MHz is targeted in downlink to achieve peak data rate of 1 Gbps. [20, 21]

There are three basic types of carrier aggregation. Contiguous intra-band CA is the case when each aggregated carrier, referred as component carrier (CC), is on the same frequency band and next to each other. Non-contiguous intra-band CA is similar to contiguous with a difference that component carriers can have some spacing as long as they are on the same frequency band. When each component carrier is in different frequency band, it is called inter-band CA. Different CA types are illustrated in Figure 3. In each CA case, the bandwidth of all CCs can vary between 1.4 MHz to 20 MHz within predefined limits. [20, 21]

The scope of this thesis concentrates on inter-band CA. This type is very feasible when operators have fragmented spectrum as inter-band CA enables large bandwidths despite narrow individual bandwidths on each frequency band. Currently specified inter-band carrier aggregation schemes are for two separate downlink bands [20]. In future the use of carrier aggregation is expected to increase and number of different band combinations will be growing. It is expected that in few years also more aggregated bands will be taken into simultaneous use in downlink. This is the main motivation behind this work.

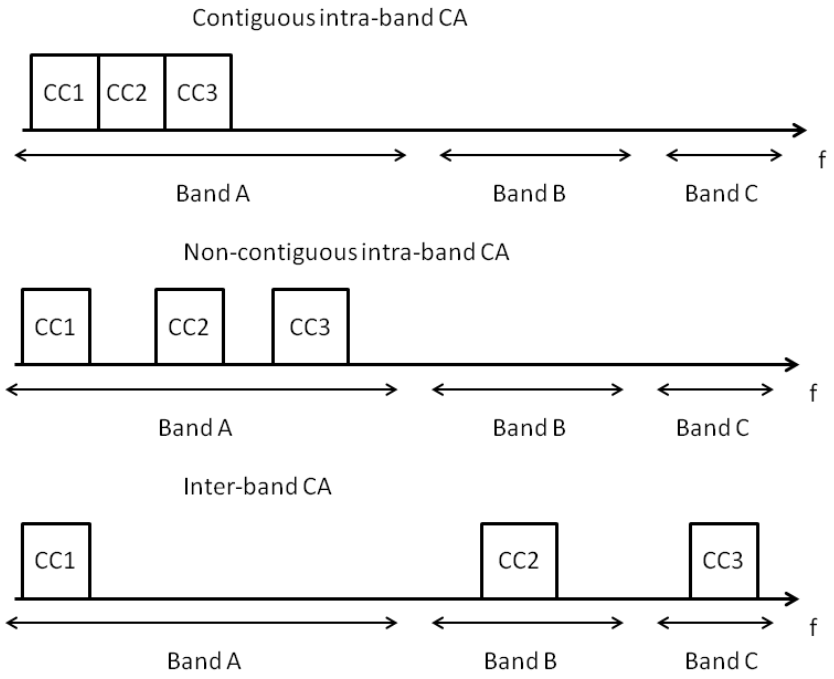

Figure 3. Illustration of different types of carrier aggregation

Because CA requires multiple frequency bands used at the same time, RF front end designers are facing a new problem. Front end must be arranged in a way that the duplexers of aggregated carriers are not loading each other through the same switch which connects multiple duplexers to antenna. Depending on which bands are aggregated this can be solved by different means. In Figure 4 an example of block diagram of RF front end suitable for three band carrier aggregation is shown. If only one carrier is aggregated from LB, MB and HB, all active duplexers are separated by either diplexer (LB-MB) or they are connected to different antenna (HB). The simplest solution to separate LB, MB and HB duplexers without additional diplexer would be to use third antenna element so that all bands would have their own antenna.

However, if two or more aggregated carriers are connected to the same antenna, for example MB, techniques described above cannot be applied. If for example bands

2 and 4 were used in CA, their duplexers would load each other through MB switch which would destroy their matching, cause additional losses and also reduce the modularity of the front end [22]. This problem can be solved by replacing duplexers of bands 2 and 4 with quadplexer like shown in Figure 4. Similarly, if HB and MB frequencies are covered by single antenna, quadplexers are needed as diplexer cannot separate closely spaced bands 30 and 1. In this case number of needed quadplexers is equal to the number of CA combination pairs in MB and HB.

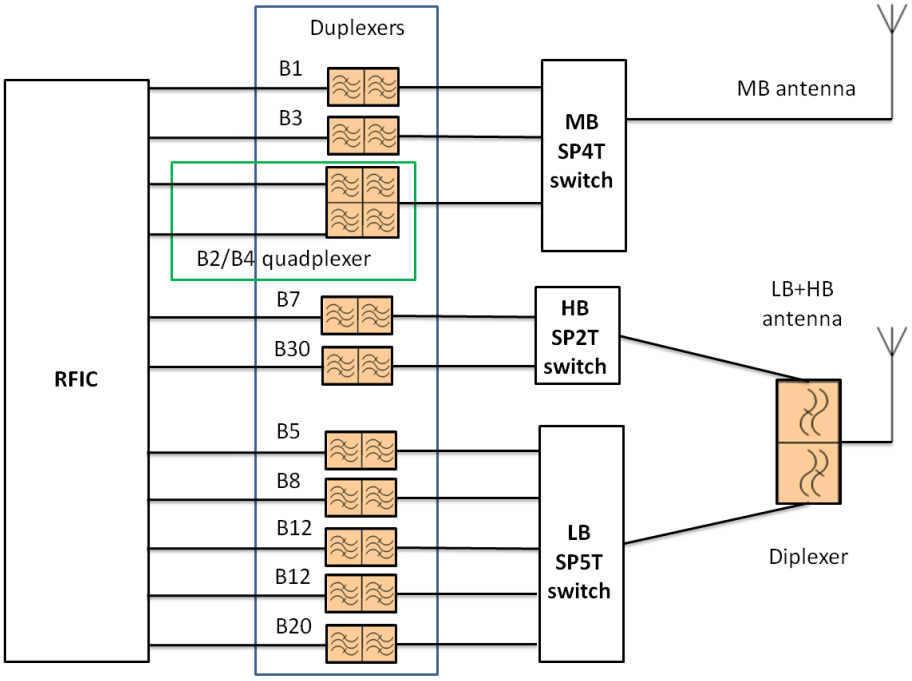

Figure 4. RF front end block diagram suitable for three band CA. Separate RX/TX connections between RFIC and duplexers are not shown.

Purely from the antenna design point of view, carrier aggregation does not change anything. Antenna designer still tries to create antennas meeting the specifications over certain frequency range with minimal volume. However, CA sets requirements for RF front end which also echo to antenna design. These requirements predetermine the number of antenna feeds and thus also dictate what kinds of antenna configurations are available to start with. Additionally it is necessary to match all bands supporting CA simultaneously which may restrict the usage of tuners. Finally, due to different antenna solutions requiring different front end configurations, total efficiency of each combination of antennas and front end must be compared to get the idea which configuration is the best.

5. PERFORMANCE REQUIREMENTS FOR SOLUTIONS

Required 3GPP operating bands and frequencies for the device designed in this thesis are illustrated in Table 1. Bands requiring CA support are darkened and others are considered roaming bands which do not need to be matched simultaneously as carrier aggregation support is not necessary for them. In carrier aggregation sense required operation is such that the device has to be able to receive from three different frequency bands simultaneously while transmitting with a single frequency. Band configuration is also such that one aggregated carrier is from low band, second from mid band and third from high band. No other combinations are considered in this thesis even though they exist [20]. From Table 2 can be seen all the required combinations of aggregated carriers. It illustrates the bands that need to be matched at the same time. It is to be noted that only one band at a time is needed from LB and MB.

Table 1. Required band coverage

		UL		DL	
		Low [MHz]	High [MHz]	Low [MHz]	High [MHz]
LB	Band 12	699	716	729	746
	Band 13	777	787	746	756
	Band 5	824	849	869	894
	Band 8	880	915	925	960
	Band 20	832	862	791	821
MB	Band 4	1710	1755	2110	2155
	Band 3	1710	1785	1805	1880
	Band 2	1850	1910	1930	1990
	Band 1	1920	1980	2110	2170
HB	Band 30	2305	2315	2350	2360
	Band 7	2500	2570	2620	2690

CA support required

Roaming band

Table 2. Required CA combinations

	LB	MB	HB
Band	12	4	30
	12	2	30
	5	4	30
	5	2	30

Design target for antenna matching in this work is -6 dB which has become widely used target in mobile antenna design [23, 24, 25]. However, nowadays even worse than -5 dB is acceptable if antenna is otherwise working well enough. To achieve better total efficiency slightly degraded matching is allowed. Number of matching components is targeted to be lower than 6, preferably 4 for each antenna. Tunable components may be used to meet the specifications. Allowable decrease in matching due to hand grip is approximately 1 dB so that -4 dB matching is still acceptable.

Efficiency targets are different for different bands. LB efficiency is targeted to be better than -5 dB. On higher bands goal is set to -3 dB. In the presence of hand efficiency degradation of at most 6 dB at LB and 10 dB at MB and HB is expected.

To ensure good MIMO performance ECC should be under 0.5 in LB and less than 0.2 in MB and HB. However, ECC around 0.6 is acceptable in LB because very simple model often gives worse results than real products with complex geometries. Multiplexing efficiency is used only to compare MIMO performance and it has no specific target.

RF front end configuration used in this thesis has three separate antenna switches, see Figure 4. This allows both the usage of separate antenna elements for all bands, and different combinations of common antenna elements. As mentioned earlier, LB can be separated from HB or MB with diplexer which allows LB to coexist with MB or HB in the same antenna. On the other hand, MB and HB must have separate antennas if use of quadplexers is not desired.

6. SIMULATION MODELS AND MATCHING CIRCUITS FOR DIFFERENT ANTENNA SOLUTIONS

Simulation models were created using commercial 3-dimensional (3D) electromagnetic field simulator software called Microwave Studio (MWS) by CST which allows creation of complex electromagnetic structures. First step before simulations was to create suitable simulation model of the mobile device. In this thesis harshly simplified model was used as the scope of this work does not require detailed analysis in actually working device and simulations are much faster without excessively precise 3D model. Also, the number of materials used in model was minimized for the same reason.

Outer dimensions of the model are 141x70x7mm^3 which is around typical size for the touchscreen devices today. Front side is covered by 1 mm thick display glass. Other outer surfaces are plastic with equal thickness. Inside the model the volume for antennas is reserved in both ends. Otherwise two large steel blocks inside the device cover the space. Metallic blocks model back panel of display and battery. However, battery block is much larger than in reality as it also models other metal components inside the device, for example the electromagnetic compatibility (EMC) -shielding on the printed circuit board. These metals blocks also form the ground plane for antennas. Outlook of the model is visualized in Figure 5 which shows the plastic cover in green and the display glass in blue color.

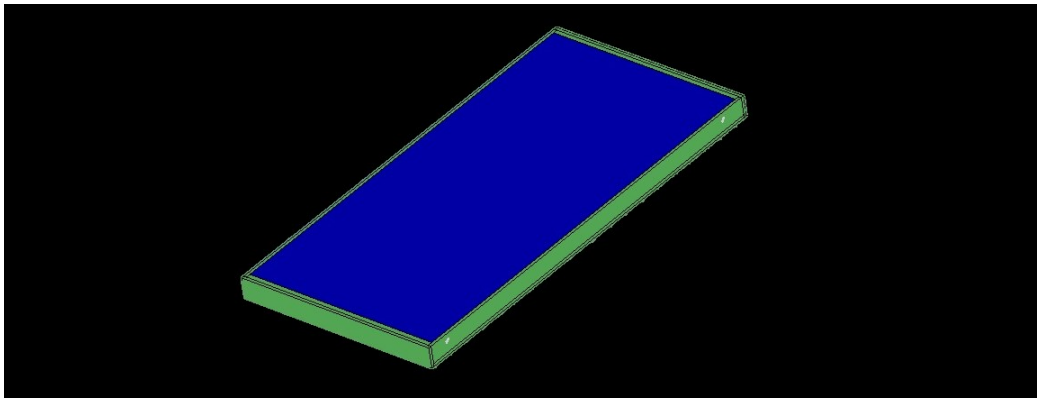

Figure 5. Outline of the used phone model.

Antenna region of the model is such that antennas itself are located just under the plastic cover on top of antenna substrate made of plastic. Antenna feeds are located on FR4 PCB material. Radiators and feeding strips are made of thin copper layer, in other words copper thickness is set to zero. Distance from antenna elements to the ground plane, i.e. antenna clearance was targeted to be 8.5 mm in main antennas and 8 mm in MIMO antennas if possible. Side cut of the model is shown in Figure 6

which illustrates the empty space reserved for antennas at both ends of the models. It can also be seen that metallic display back panel and excessive metal plate modeling battery and other metallic structures inside the device consume most of the space inside the device. Metallic structures are yellow in figures.

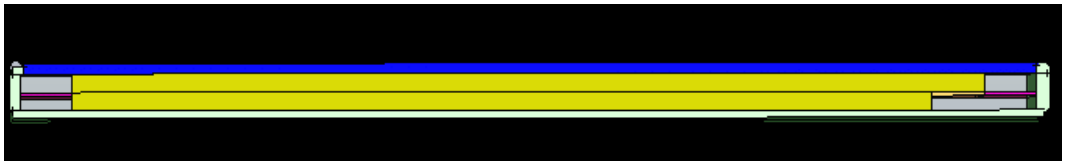

Figure 6. Side cut of the phone model.

Both main and MIMO antenna regions are illustrated more accurately in Figure 7. Antenna clearances are measured as shortest distances from yellow metal to the farthest edge of the green antenna carriers where antennas are located. Purple model block is FR4. Antenna feeding points are on top of FR4 layer at the intersection of FR4 and metal next to it. All dimensions of the model without antenna elements are shown in Table 3. In Figure 7, plastic cover parts at side, top and bottom edges are not shown.

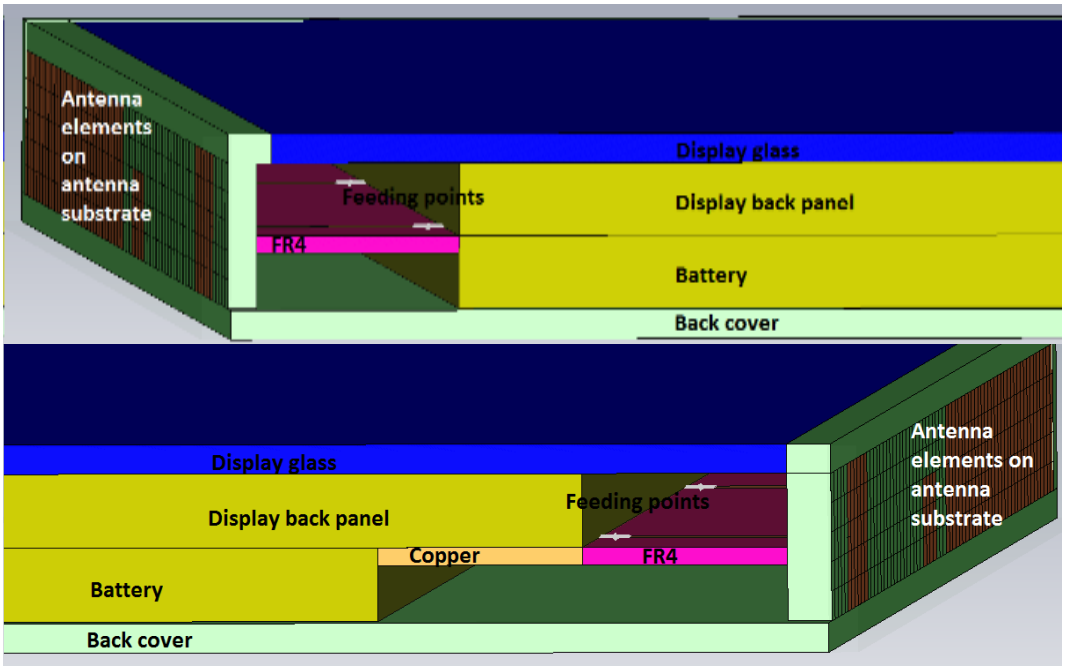

Figure 7. Main (lower) and MIMO (upper) antenna regions of the phone model.

Key characteristics of the used materials are shown in Table 4. For insulators relative permittivity and permeability with loss tangent are shown. Conductivity is used as a metric to measure the quality of conductive materials.

Table 3. Dimensions of the phone model without antenna elements

Block	Width [mm]	Height [mm]	Thickness [mm]	Material
Model dimensions	70	141	7	-
Antenna carrier (Main antenna)	68	1.5	5	ABS plastic
Antenna carrier (MIMO antenna)	68	1	5	ABS plastic
Battery	68	115.5	2.5	Stainless steel
Display glass	68	136	1	Glass
Display metal	68	122.5	2.5	Stainless steel
FR4 (Main antenna)	68	7	0.6	FR4
FR4 (MIMO antenna)	68	7	0.6	FR4
PCB copper (Main antenna)	68	7	0.6	Copper
Plastic cover	-	-	1	ABS plastic

Table 4. Key characteristics of the materials used in the model

Material	Color	Purpose	Relative permittivity (insulators) or conductivity (conductors)	Relative permeability	Loss tangent
Insulators			ε_r	μ	tan δ
ABS Plastic	Green	Covers, antenna carrier	3.2	1	0.01
FR4	Purple	Antenna PCB	4.3	1	0.025
Glass	Blue	Display	7.5	1	0.03
Conductors			σ [S/m]		
Copper	Gold	Antennas	$5.88*10^7$		
Stainless steel	Yellow	Battery, display back, lossy metals	$1.39*10^6$		

6.1. Matching components

After the initial simulation with CST MWS, S-parameters were exported to second commercial software called Optenni Lab. Optenni Lab is used to match the antenna input impedance obtained from MWS to 50 ohms by optimizing the transducer power gain through the required frequency range. It can also be used to do quick analysis of the performance of the simulated antenna after matching.

With Optenni Lab one can calculate bandwidth potential with adjustable return loss specification for simulated antennas. This is done by sweeping through frequencies and conjugate matching at all frequency points with two lossless

matching components. Output from this calculation gives a graph illustrating maximum achievable bandwidth at certain center frequency. [26, 27]

Also, worst case electromagnetic isolation between simulated ports can be calculated with Optenni Lab. Worst case situation is created by sweeping through frequencies and matching both ports with complex conjugates at the same time. In real case the isolation is equal or better than this estimate as antennas are not usually matched with conjugate matching. Additional improvement of isolation is caused by resistive losses in the matching circuit. [26, 27]

After checking that the bandwidth potential and electromagnetic isolation are acceptable, one can start creating matching circuits for the antennas. Optenni Lab enables easy matching circuit generation. One can select specific communication systems to be matched or specify the frequencies to be matched. Efficiency target can be set as well as the number of matching components in the matching circuit. Real components can be used from libraries. In this work however, specifications for lossy components were set to be same for all components. Used value for quality factor (Q) for inductors is 60 and for equivalent series resistance (ESR) for capacitors 0.3 ohm, both at 1 GHz frequency. Resistive losses of inductors can be derived from

$$Q = \frac{2\pi f L}{R}, \tag{15}$$

where Q is the quality factor, f frequency, L inductance and R parasitic series resistance of inductor [28].

One can also define specific stop bands for matching circuits to increase isolation between different antennas. After specifications are set, Optenni Lab automatically calculates multiple matching circuit options. Designer can select the optimal and export it back to CST for final simulations. [26]

Block diagram of different simulation phases is shown in Figure 8. Initial full wave simulation of the model is done in MWS. The resulting S-parameters, or raw S-parameters, are imported to Optenni Lab which is used to optimize matching circuits for each port. S-parameters of each matching circuit are then imported to MWS which performs the final system simulation and post processing.

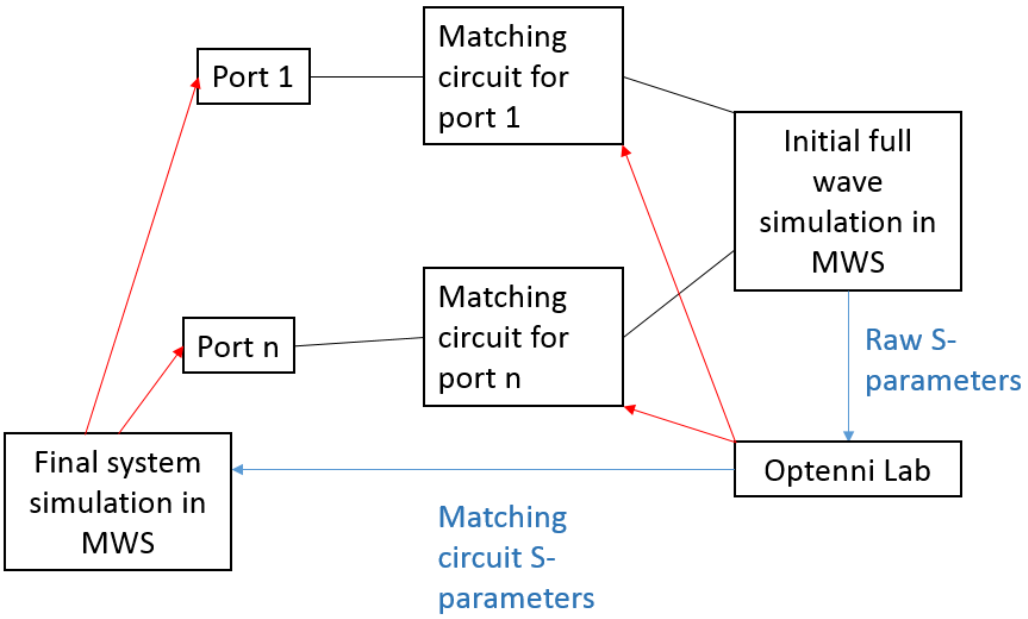

Figure 8. Block diagram of simulation phases.

6.2. Separate antenna elements for LB, MB and HB (Design 1)

The first model has separate antenna elements for LB, MB, HB and their MIMO antennas. A total of six antenna elements and feeds are needed. All feeding strips have 1 mm width. The main antenna elements are located on bottom part of the model and MIMO antennas on top part of the model. Both main and MIMO antenna structures of the design are shown in Figure 9. Size and volume of the elements are gathered in Table 5.

With a single tunable inductor in matching circuit of both LB elements all bands can be matched to meet all requirements with desired clearances. Main antenna requires four and MIMO antenna needs three separate inductor values for tuner. Tuning is implemented by using ideal SPxT switches to connect the desired inductor to the matching circuit. Matching circuits for all antennas are illustrated in Figure 10 and in Figure 11. In LB main antenna used tuning inductances are 10 nH (Band 8), 14.1 nH (Bands 5 and 20), 20 nH (Band 13) and 25.1 nH (Band 12). Inductances used to tune LB MIMO antenna are 10.5 nH (Bands 5 and 8), 15.8 nH (Band 20) and 21.4 nH (Bands 12 and 13). MB and HB antennas do not require tunable matching circuits.

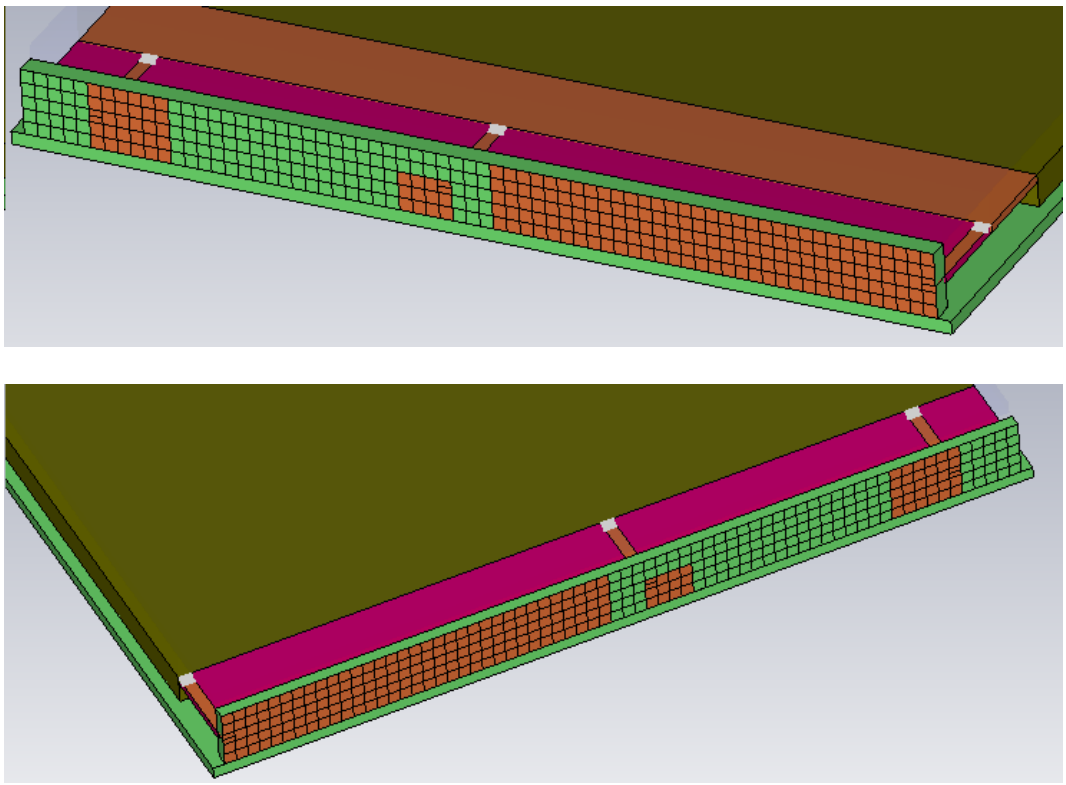

Figure 9. Main (upper) and MIMO (lower) antennas of solution with separate antenna elements. Square size 1 x 1 mm.

Table 5. Dimensions and volumes of the antenna elements in design 1

	Width [mm]	Height [mm]	Clearance [mm]	Volume [mm^3]	Feed distance from the nearest edge [mm]
LB Main	33	5	8.5	1402.5	0
LB MIMO	33	5	8	1320	0
MB Main	6	5	8.5	255	5
MB MIMO	6	5	8	240	5
HB Main	4	3	8.5	102	31
HB MIMO	4	3	8	96	31

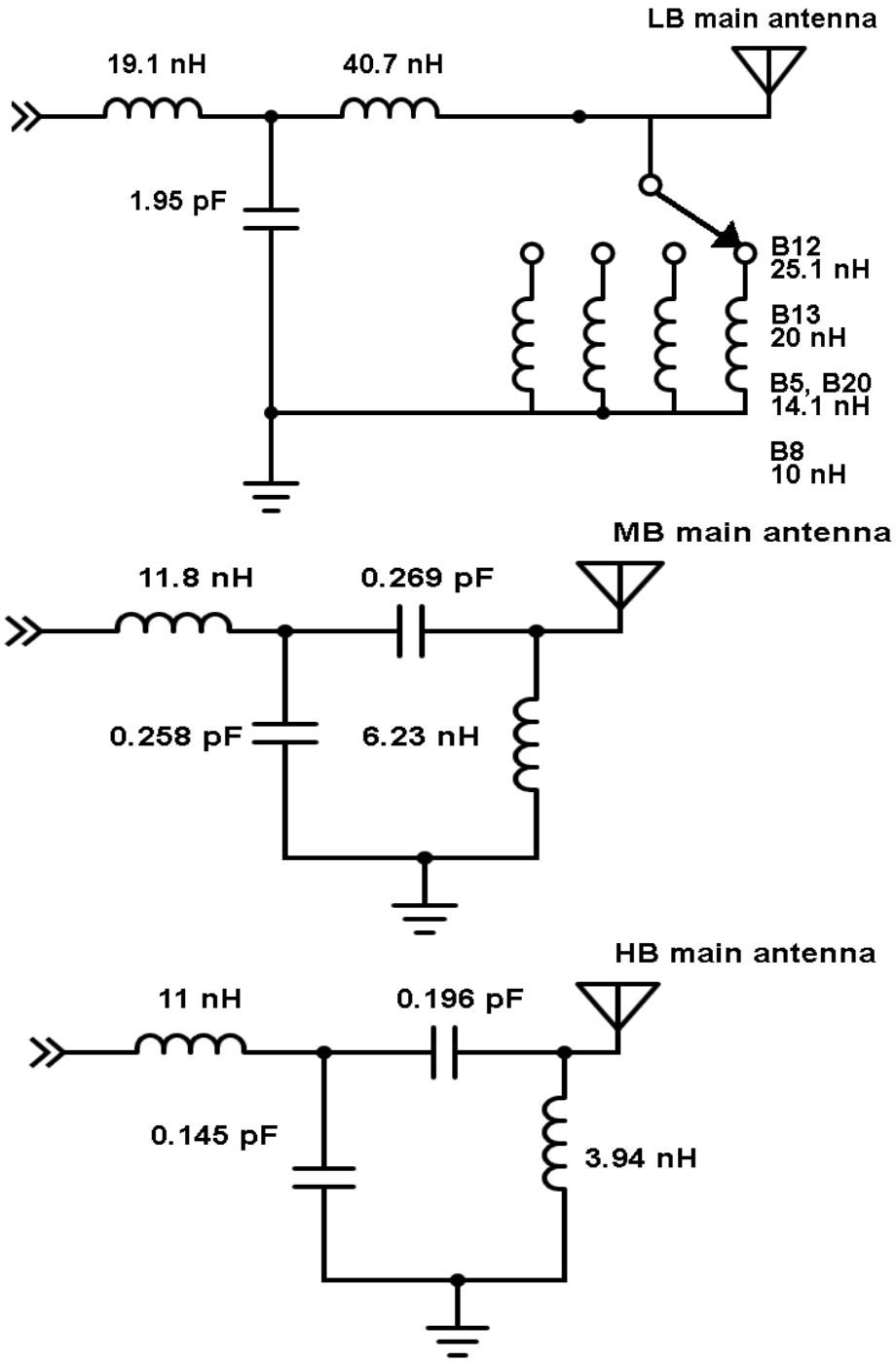

Figure 10. Matching circuits of the main antennas in design 1.

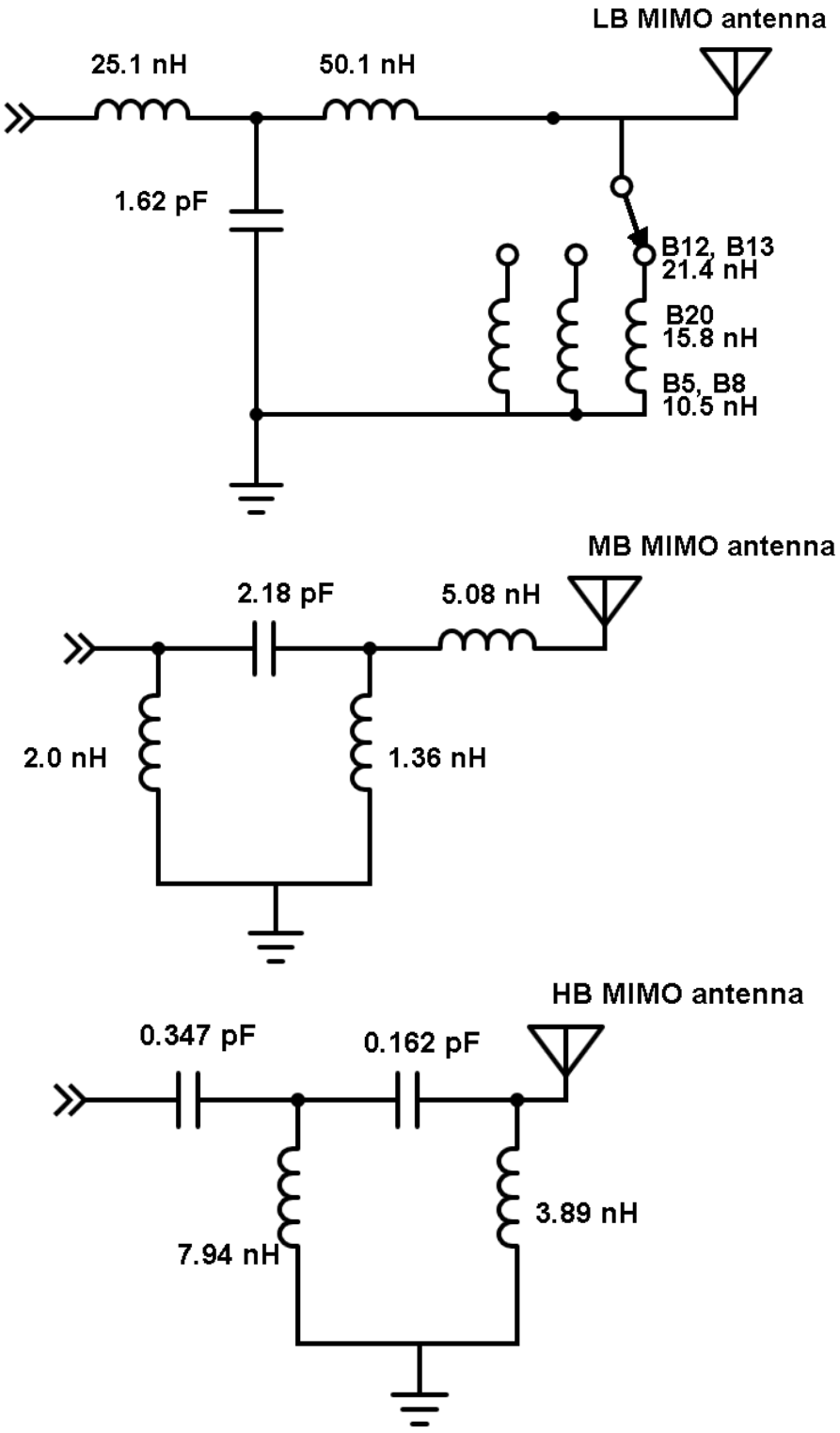

Figure 11. Matching circuits of the MIMO antennas in design 1.

One possible RF front end configuration to this design is shown in Figure 12. The front end consists of duplexers for each band and three antenna switches for selecting the bands. In this front end diagram the possible CA pairing of bands 2 and 4 is not taken into account. This configuration has separate transmission lines for all

elements, a total of six transmission lines when also MIMO antennas are included. An alternative front end configuration for design 1 is shown in Figure 13. This configuration has common transmission line for MB and LB antennas. Combining the feeds requires two additional diplexers, one at both ends of the transmission line. Thus, comparing to front end with separate transmission lines, this configuration saves space by removing two transmission lines but loses efficiency as two diplexers have a loss of approximately 0.8 dB. Diplexers can separate either MB or HB from LB, so depending for example which antenna is more efficient, designer can select which antenna has direct transmission line feed and which is routed through the lossy diplexers.

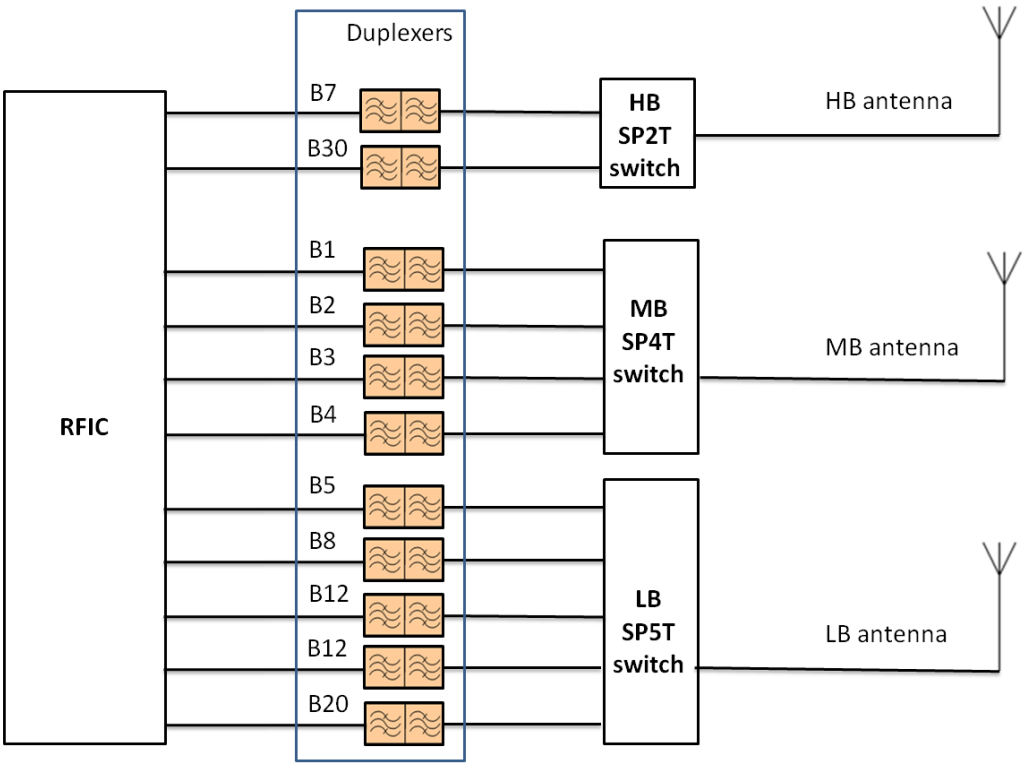

Figure 12. Block diagram of RF front end for design 1. Separate RX/TX connections between RFIC and duplexers are not shown.

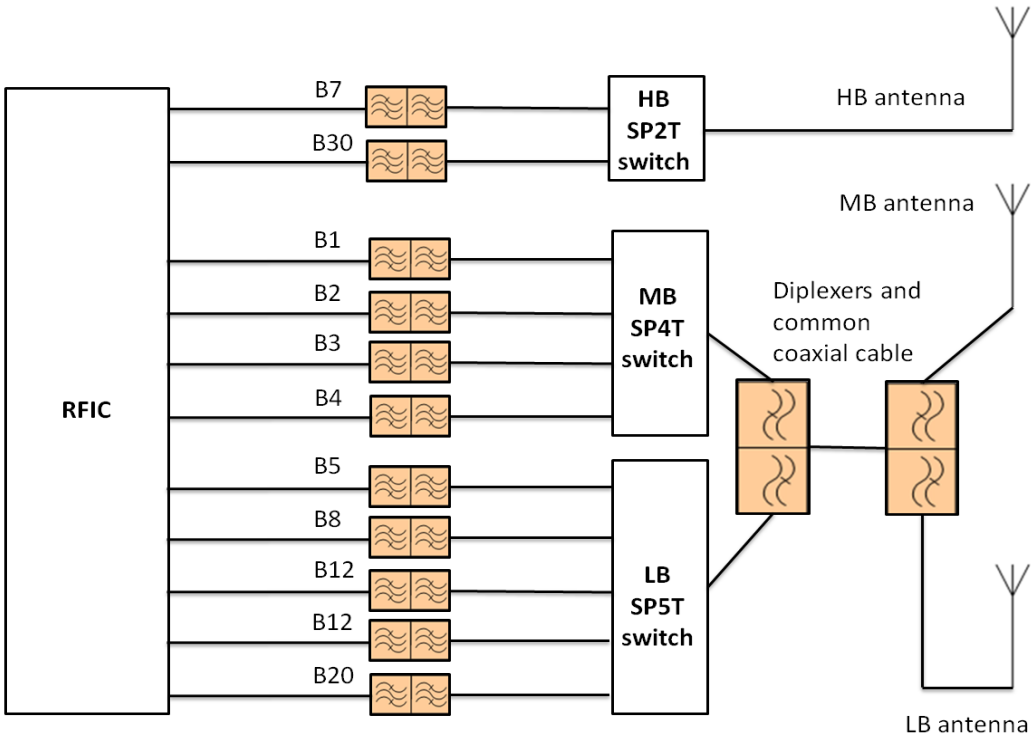

Figure 13. Block diagram of RF front end for design 1 with reduced number of coaxial cables. Separate RX/TX connections between RFIC and duplexers are not shown.

6.3. Common antenna element for LB and HB with separate MB element (Design 2)

The second model consists of a total of four antenna elements. Main and MIMO antenna elements have similar locations to prior model with separate elements. In this model the RF front end has two feeds. One common feed for LB and HB which share a common antenna element and one feed for separate MB element. Used MB element is exactly the same as in the design with three separate antennas expect it is on the opposite bottom corner of the device. To successfully match both high and low bands at the same time, larger antenna element and wider antenna clearance were needed comparing to design using separate LB and HB antenna elements. Additional metal free space required for increased clearance was created by shortening the display metal and battery. Space was filled with bigger FR4 blocks at both ends of the model. Requirements were met with antenna clearances of 10 and 9 mm for main and MIMO antennas, respectively. To enhance HB performance from the LB element similar to one used design of the section 6.2 the feeding point was moved from the edge of the device to an offset of 12 mm which was by simulations found to be optimal. Visual illustrations of antenna structures are shown in Figure 14. Physical dimensions and calculated volumes are gathered in Table 6.

Using tuners with the common LB and HB element was found to be much more difficult as tuning the other band often causes detuning of the other. However, sufficient performance was achieved through the whole frequency range by using tuning circuits consisting of six components in both main and MIMO antennas. In both antennas tuning is done by using SP2T switch between two different inductances. Matching circuits with components values are presented in Figure 15 and Figure 16. Used tuning inductances in LBHB main antenna are 13.2 nH (Bands 12, 13, 20, 5, 7 and 30) and 8.71 nH (Bands 8 and 7). LBHB MIMO antenna is tuned with inductances of 14.8 nH (Bands 12, 13, 20, 30 and 7) and 10.7 nH (Bands 5, 8, 30 and 7). MB elements do not require tuners.

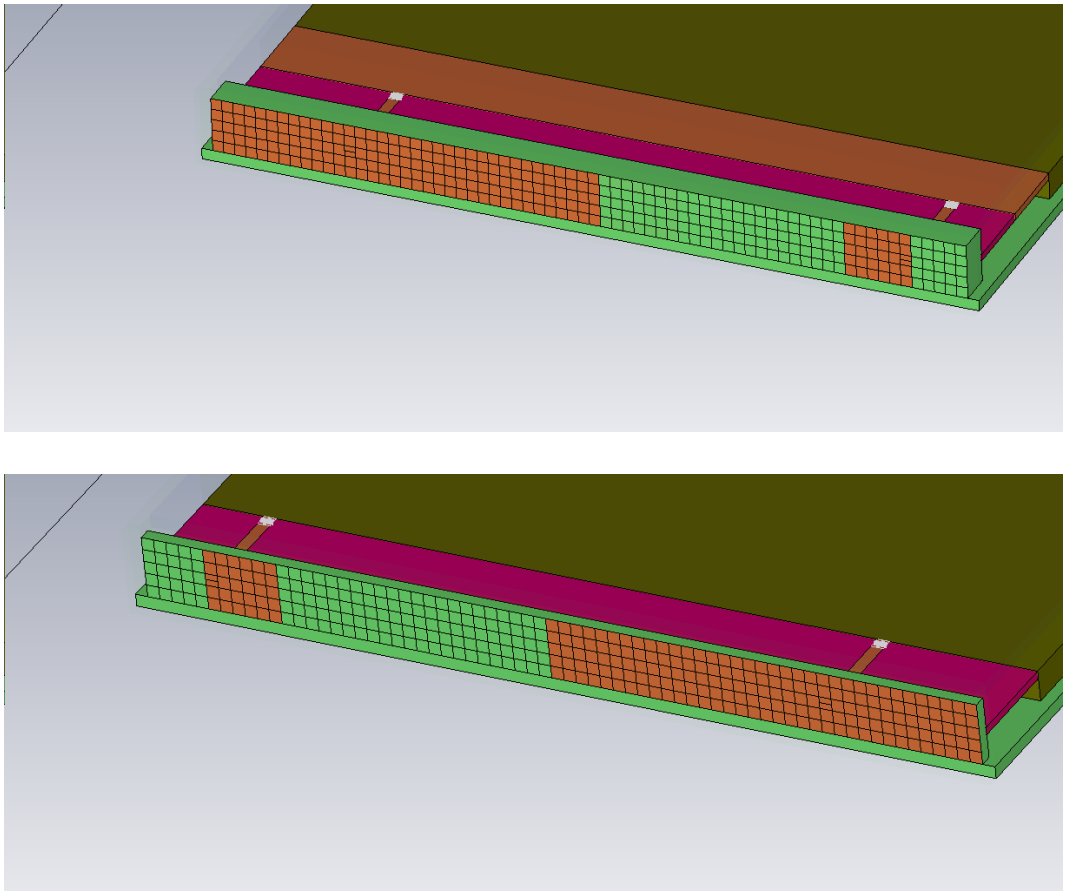

Figure 14. Main (upper) and MIMO (lower) antennas of solution with common LB and HB elements. Square size 1 x 1 mm.

Table 6. Dimensions and volumes of the antenna elements in design 2

	Width [mm]	Height [mm]	Clearance [mm]	Volume [mm^3]	Feed distance from the nearest edge [mm]
LBHB Main	35	5	10	1750	12
LBHB MIMO	35	5	9	1575	12
MB Main	6	5	10	300	5
MB MIMO	6	5	9	270	5

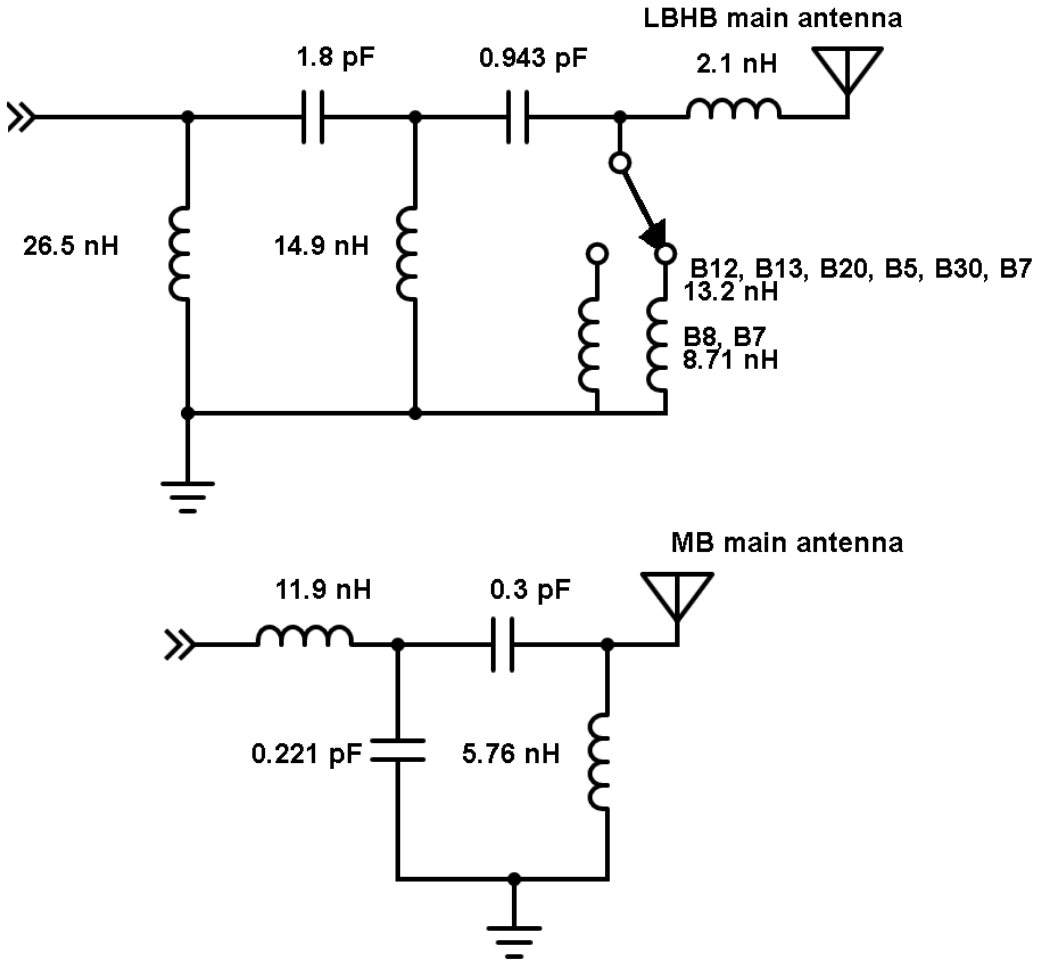

Figure 15. Matching circuits of the main antennas in design 2.

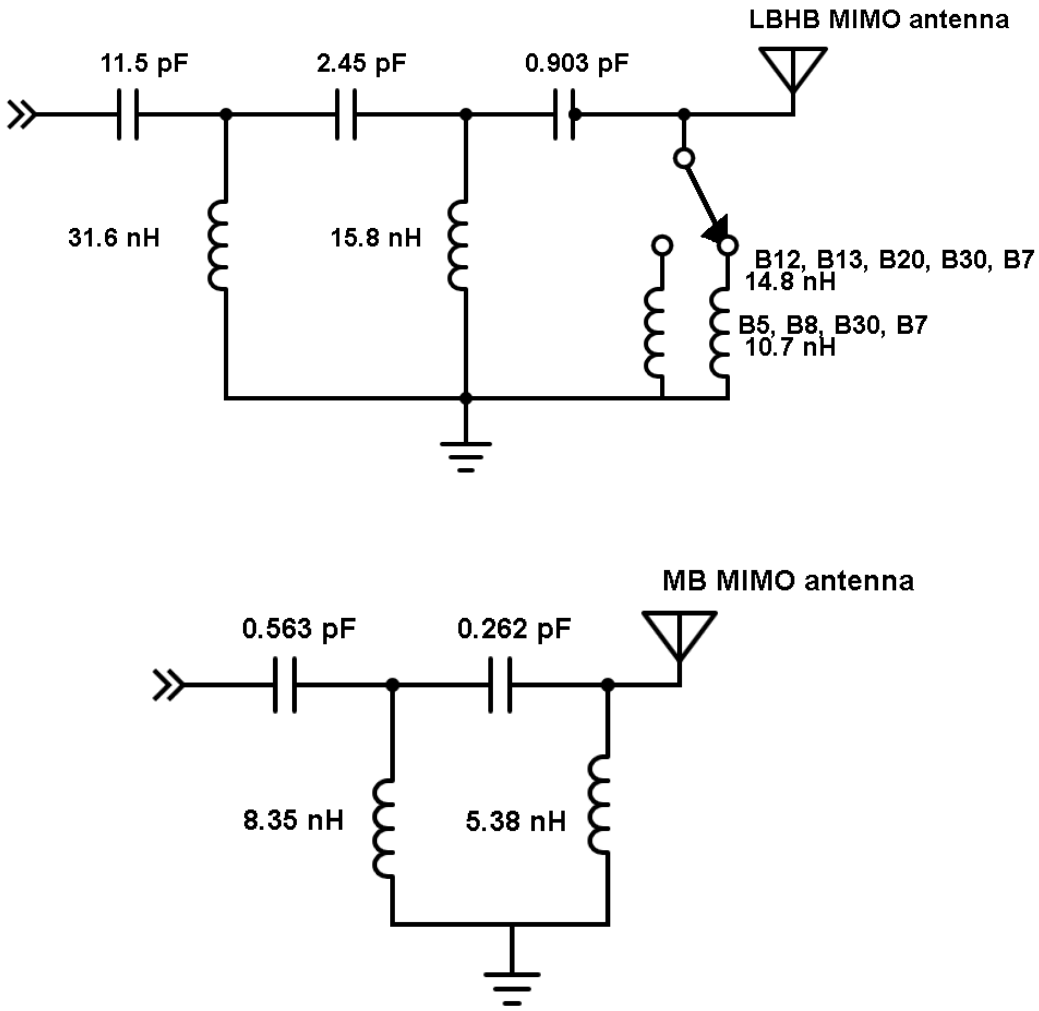

Figure 16. Matching circuits of the MIMO antennas in design 2.

RF front end configuration to this design is shown in Figure 17. The front end consists of duplexers for each band and three antenna switches for selecting the bands. In this front end diagram the possible CA pairing of bands 2 and 4 is not taken into account. Diplexer separates the simultaneously active LB and HB duplexers enabling the CA functionality. To implement this solution a total of four transmission lines is needed to connect the main and MIMO antennas to the front end.

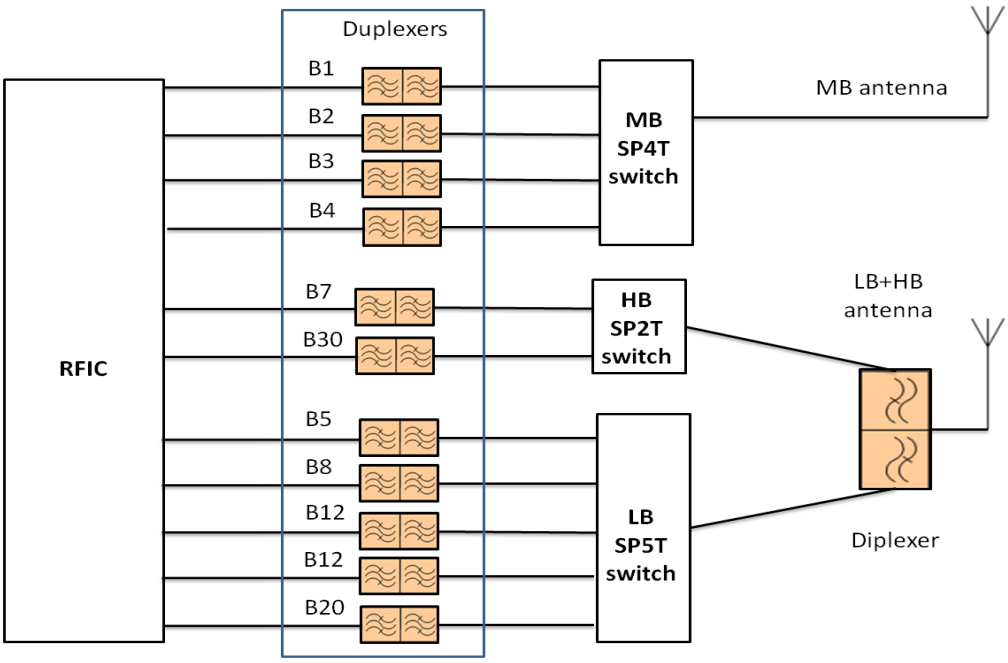

Figure 17. Block diagram of RF front end for design 2. Separate RX/TX connections between RFIC and duplexers are not shown.

6.4. Hand phantom

Performance of proposed solutions was verified by simulating the effect of human hand grip on the device. The shape, material properties and the grip from the device are standardized by the Wireless Association (CTIA) [29]. Personal Digital Assistant (PDA) grip hand is suitable for the 70 mm wide device used in this thesis. Hand grip used in simulations is modeled according to CTIA standards and left hand grip is visualized in Figure 18. Also, performance in right hand grip was simulated. Beige material in picture is the spacer used to help positioning of the device. The spacer material is not included in simulations as it is not part of real human hand.

Usually mobile phone antenna performance is affected also by the user's head. In this thesis simulations with head were left out for a couple reasons. Head mostly reduces efficiency as opposed to hand which may also detune the antennas as hand grip is very close to antennas. Also head model is rather complex and thus would have increased the simulation times significantly.

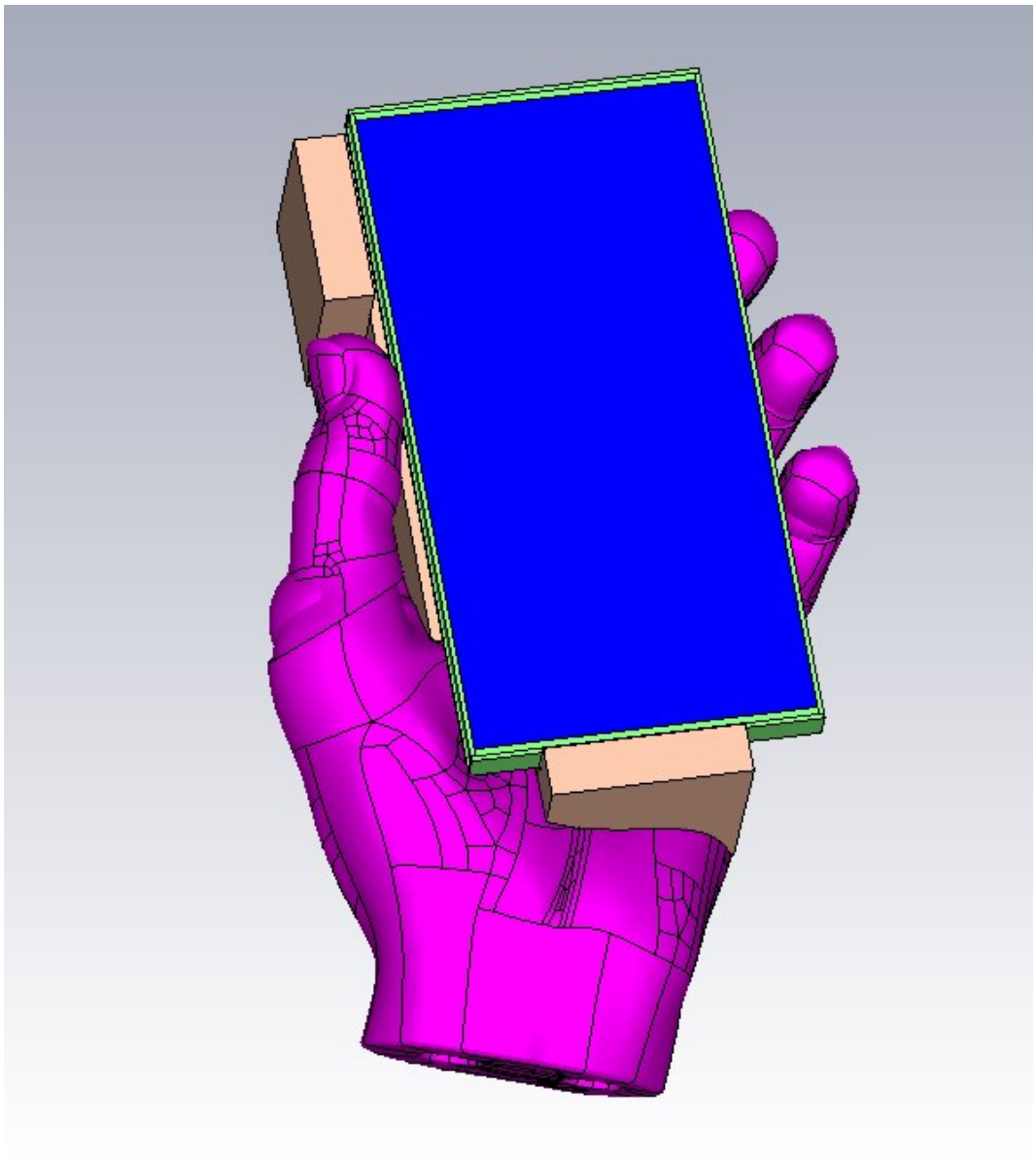

Figure 18. Hand grip used in simulations.

7. SIMULATION RESULTS OF MATCHED ANTENNAS

Final simulations were performed by using MWS after exporting the matching circuits from Optenni Lab. In this chapter the results of proposed designs are illustrated. Worst case results of all specified frequency bands for both designs are shown in tables in section 7.5.

7.1. Results of the design 1 in free space (FS)

LB main antenna matching with different tuner settings is presented in Figure 19. Markers in the curves denote the required frequency range for each tuner value. It can be seen that matching is better than -6 dB in all cases. Figure 20 illustrates the matching of main MB and HB antennas. It is also shown in Figure 20 that tuning of LB antenna affects also on HB antenna by tuning it to slightly higher frequency. This tuning improves matching on band 7 frequencies over 2.5 GHz. MB antenna matching is not affected by tuning of LB so only one curve of S_{22} is shown. Both MB and HB results are better than -6 dB if tuning of LB antenna is used to improve band 7 performance when required.

Similar graphs of MIMO antenna matching is presented in Figure 21 and Figure 22. Results of MIMO antennas are similar to the corresponding main antenna results which also meet the specifications.

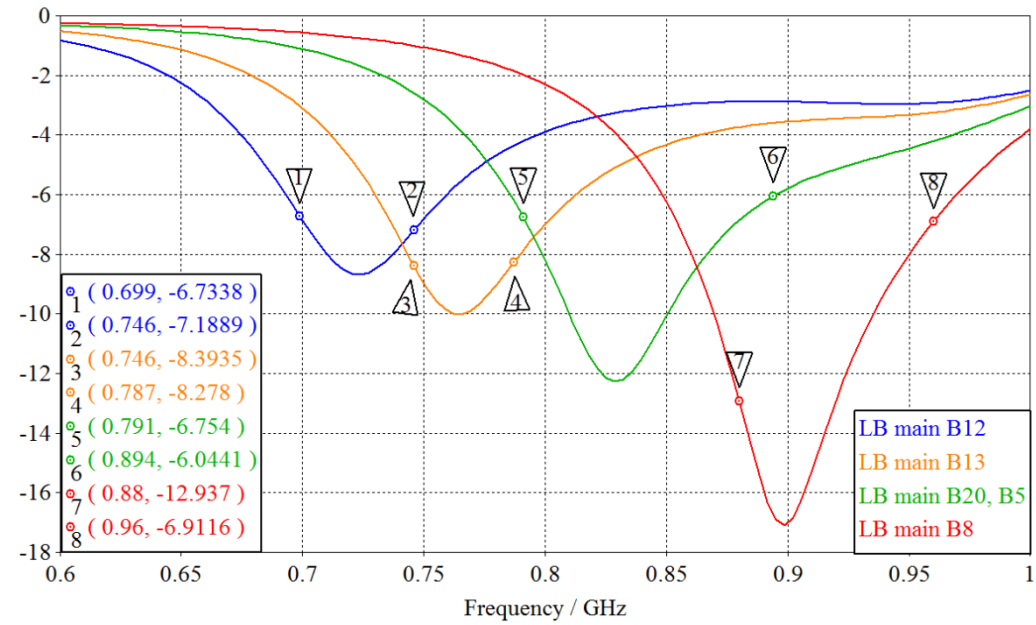

Figure 19. Design 1 LB main antenna matching with different tuner settings.

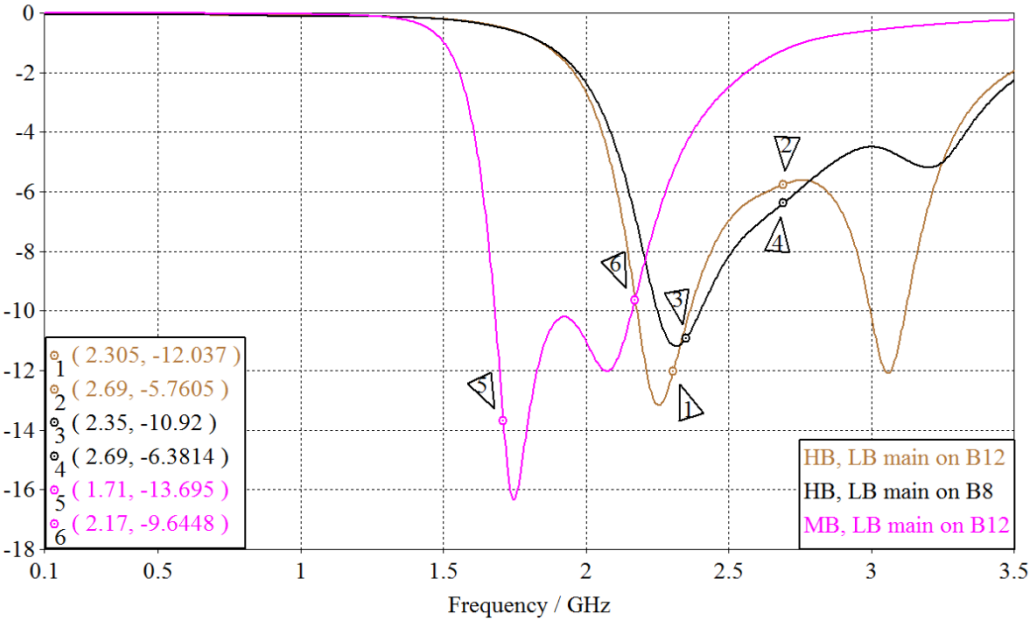

Figure 20. Design 1 MB and HB main antenna matching.

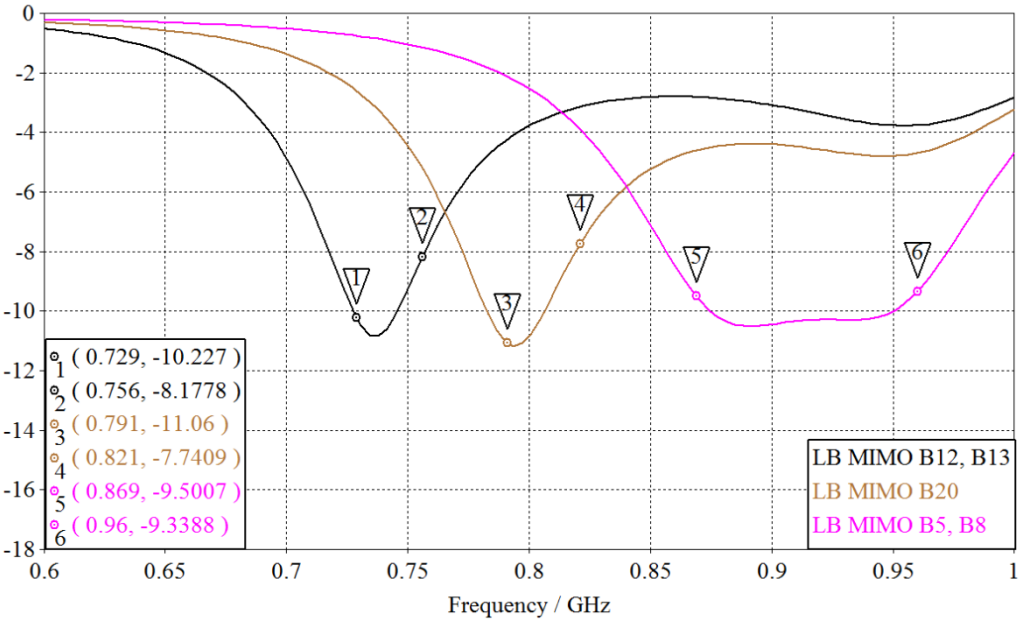

Figure 21. Design 1 LB MIMO antenna matching with different tuner settings.

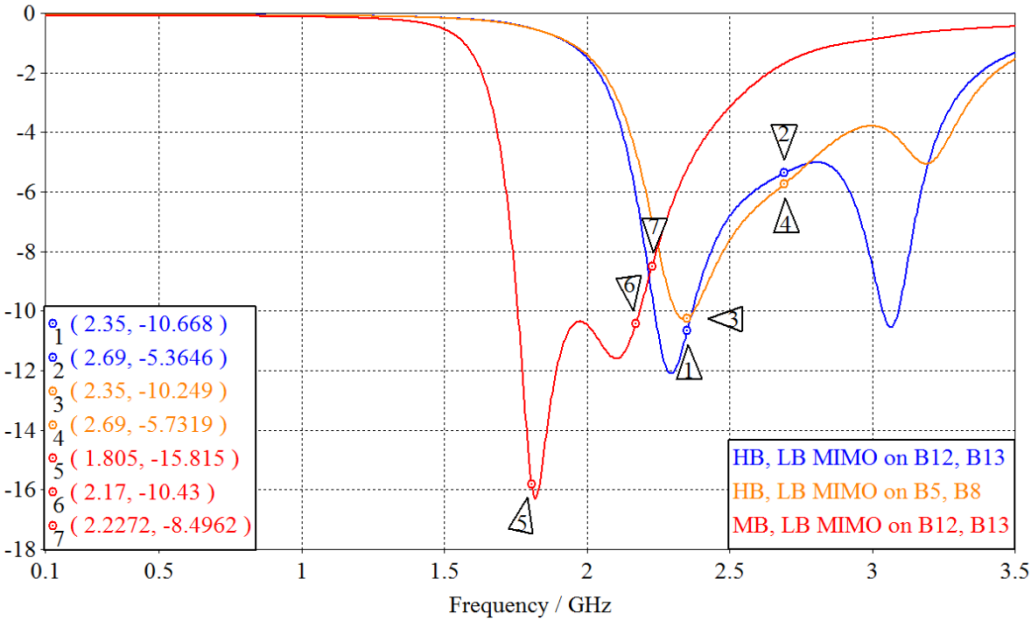

Figure 22. Design 1 MB and HB MIMO antenna matching.

Total efficiencies of the three main antennas are shown in Figure 23 where LB efficiencies with different tuner settings are shown in a single graph. Figure shows also that LB tuning causes slight changes also in HB efficiency around band 7 frequencies. Corresponding results for MIMO antennas with similar tuning effects are presented in Figure 24. Exact worst case results from each band are presented in section 7.5

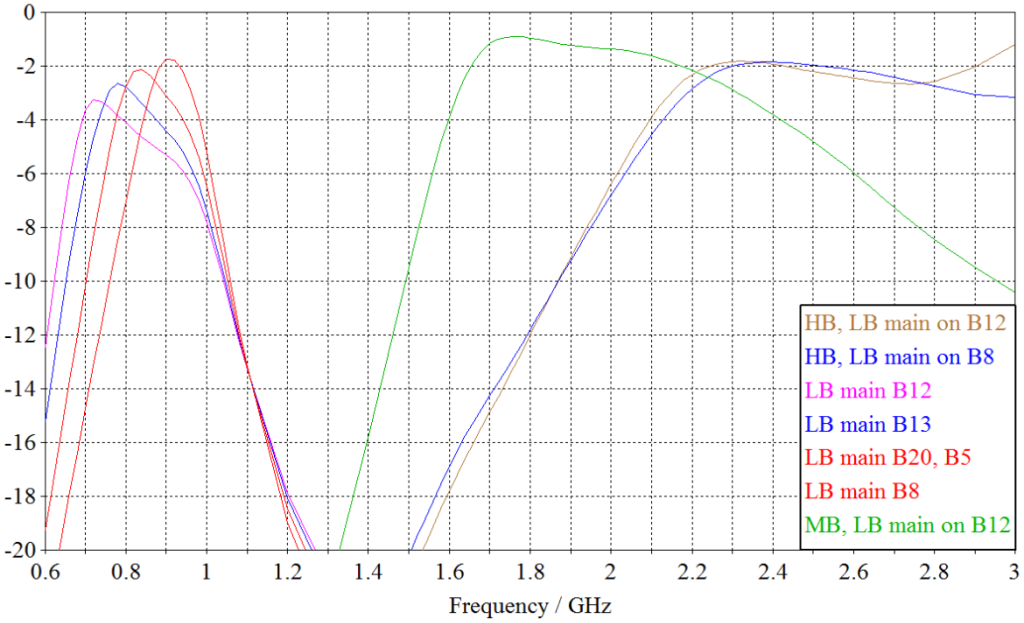

Figure 23. Design 1 main antenna total efficiencies with different LB tuner settings.

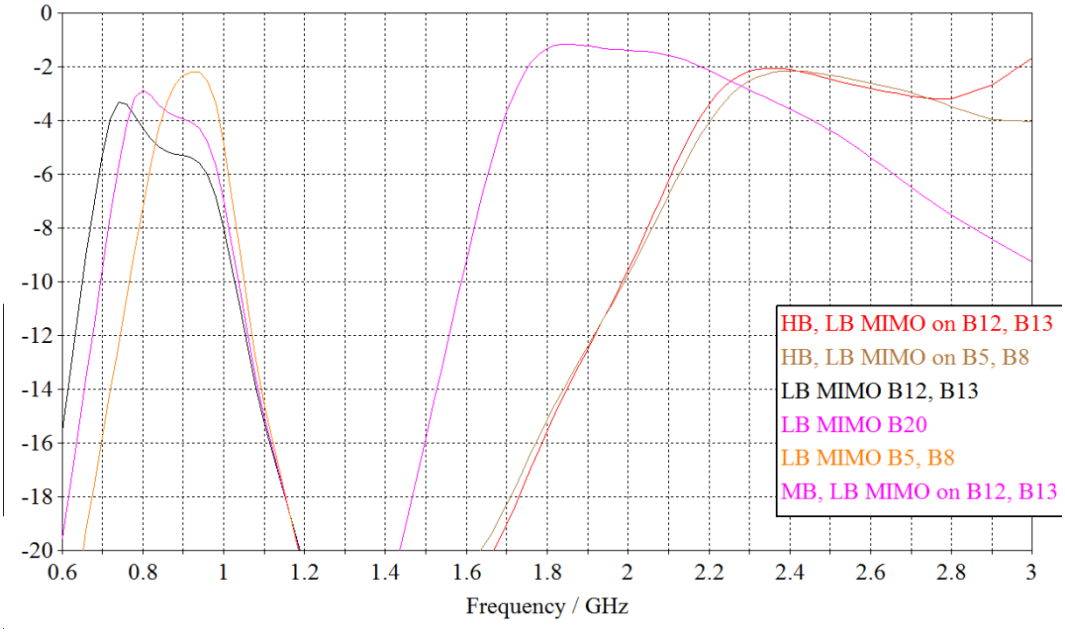

Figure 24. Design 1 MIMO antenna total efficiencies with different LB tuner settings.

MIMO performance was evaluated by simulating ECC and multiplexing efficiency of design. ECC results of each frequency band using LB antenna are shown in Figure 25. As MB and HB results are nearly zero and thus much better than required 0.2 they are not shown here. Simulations indicate that ECC target of 0.5 is met also on LB frequencies. Graphs denoting multiplexing efficiencies are shown in Figure 26. On lowest frequencies where efficiency and ECC are worst, multiplexing efficiency reaches its lowest value around -4.5 dB at 729 MHz which is the lowest frequency where MIMO is used. In MB and HB frequencies multiplexing efficiency is better than -3 dB.

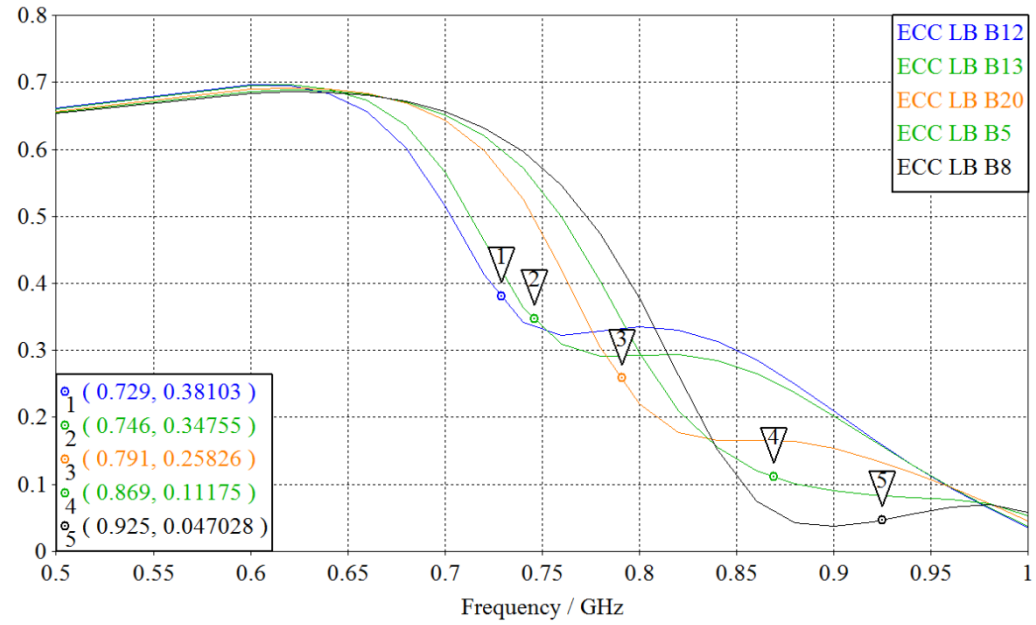

Figure 25. Design 1 ECC results.

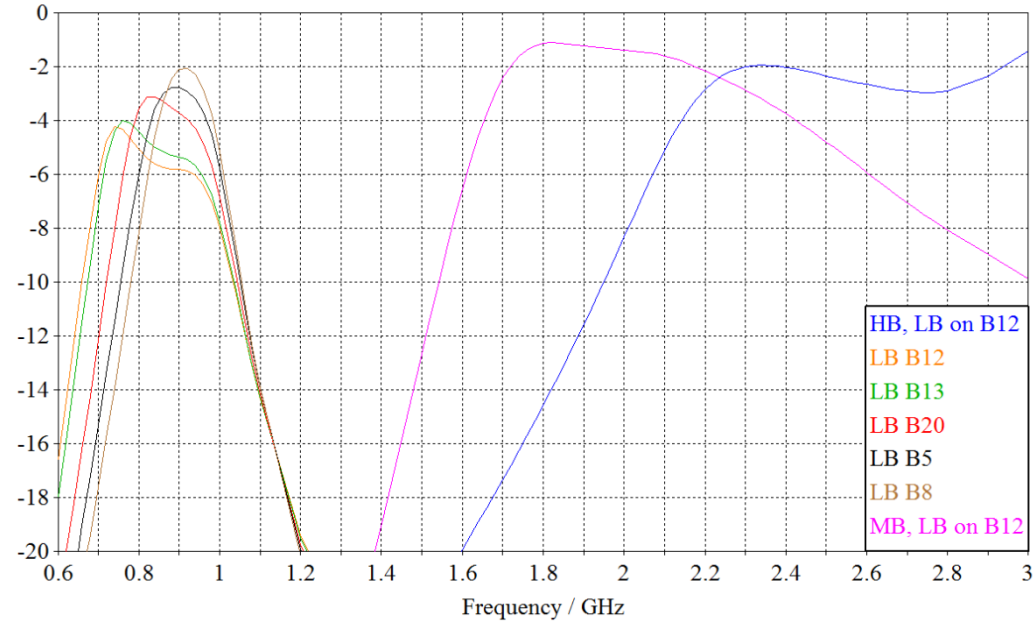

Figure 26. Design 1 multiplexing efficiencies.

7.2. Results of the design 1 in left and right hand grips (HL and HR)

Simulations results in the presence of hand model are presented next. First, in Figure 27 is comparison of the LB main antenna matching between free space, left hand and right hand grips. Markers denote the worst hand grip or free space result for each

tuner setting. Results show that left hand grip moves the LB resonance to slightly lower frequency compared to free space simulations. With the right hand grip, more wideband but weaker resonances are achieved. However, despite the different grips all LB main antenna matching results are better than -5 dB fulfilling the requirement easily.

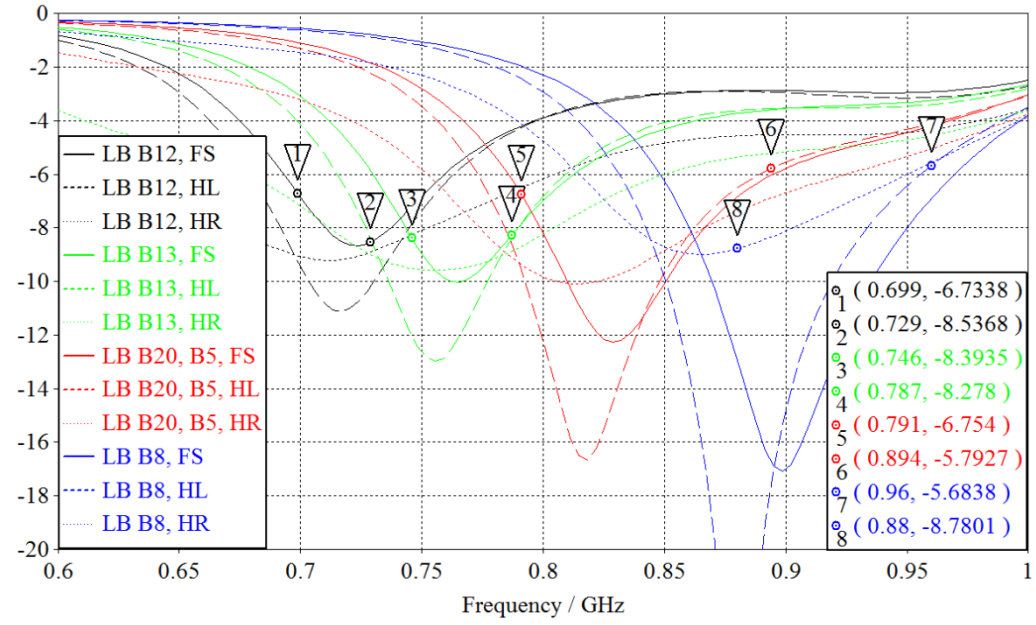

Figure 27. Matching of the design 1 LB main antenna in the presence of hand with different tuner settings.

Corresponding hand simulation results for LB MIMO antenna are shown in Figure 28 where markers illustrate the worst simulation result for each tuner position. Figure shows that LB MIMO antenna matching is clearly better than -6 dB.

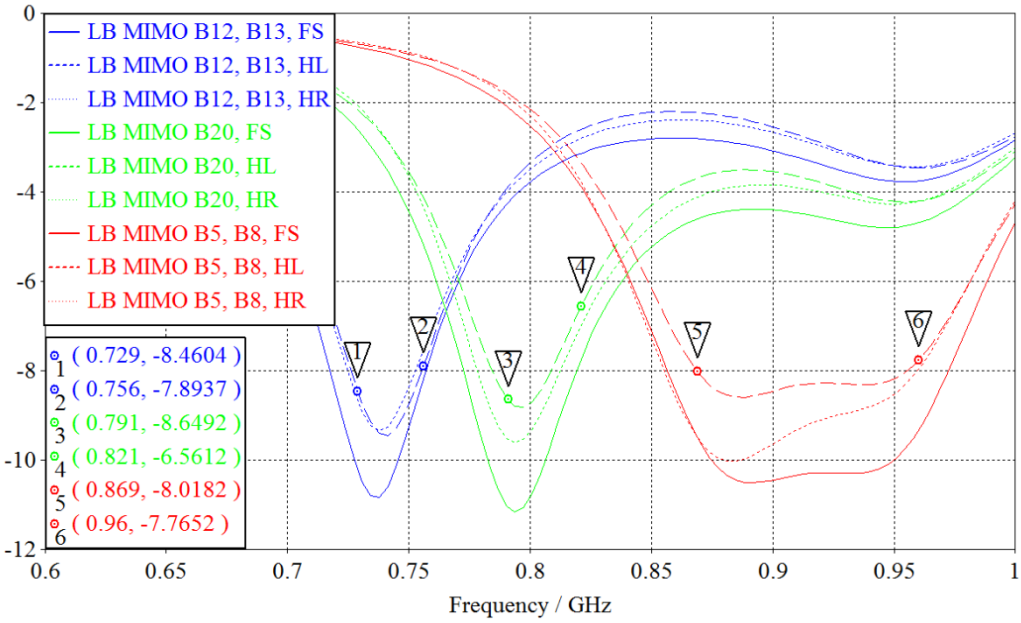

Figure 28. Matching of the design 1 LB MIMO antenna in the presence of hand with different tuner settings.

In Figure 29 is shown the comparison of MB and HB antenna matching between free space and hand simulations. Markers again highlight the worst performance in each band. While MB results are better than -5 dB in all cases, it is clear that left hand grip degrades the performance and tunes the resonance to lower frequency. HB results are shown with two extreme LB tuner settings. Band 7 is matched better when LB is tuned to band 8 with 10 nH tuning inductor. On the other hand, band 30 which is used in CA is matched well in both cases to enable CA operation without dependence to LB tuner setting. Corresponding results for MB and HB MIMO antennas are shown in Figure 30. It can be seen that MIMO antenna results are barely affected by hand grips and matching is better than -5 dB.

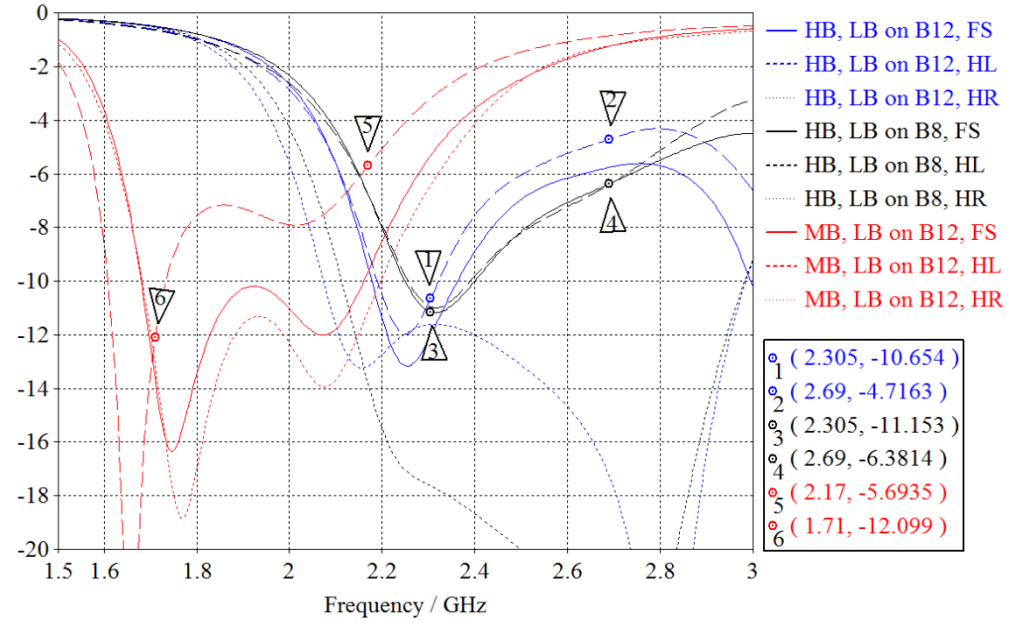

Figure 29. Matching of the design 1 MB and HB main antennas in the presence of hand.

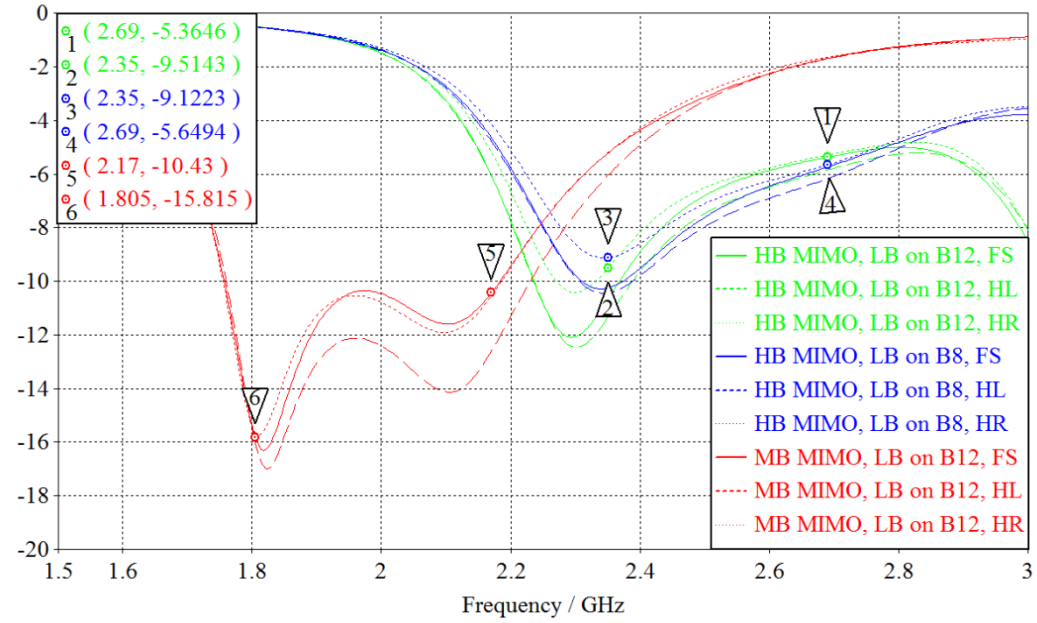

Figure 30. Matching of the design 1 MB and HB MIMO antennas in the presence of hand.

The effect of hand grip on total efficiency is illustrated next. LB antenna results are divided in two figures to show results more clearly. LB main antenna total efficiencies while antenna is tuned to bands 12, 20 and 5 are shown in Figure 31. When antenna is tuned to bands 13 and 8, results are shown in Figure 32. An

attenuation around 4 – 5 dB is observed between free space and hand simulations through the low band frequencies. Hand grip causing more attenuation varies between different tuner settings. It seems that left hand attenuates more in the lower bands 12 and 13 while right hand causes more problems on bands 5, 8 and 20. However, differences between hands are rather small.

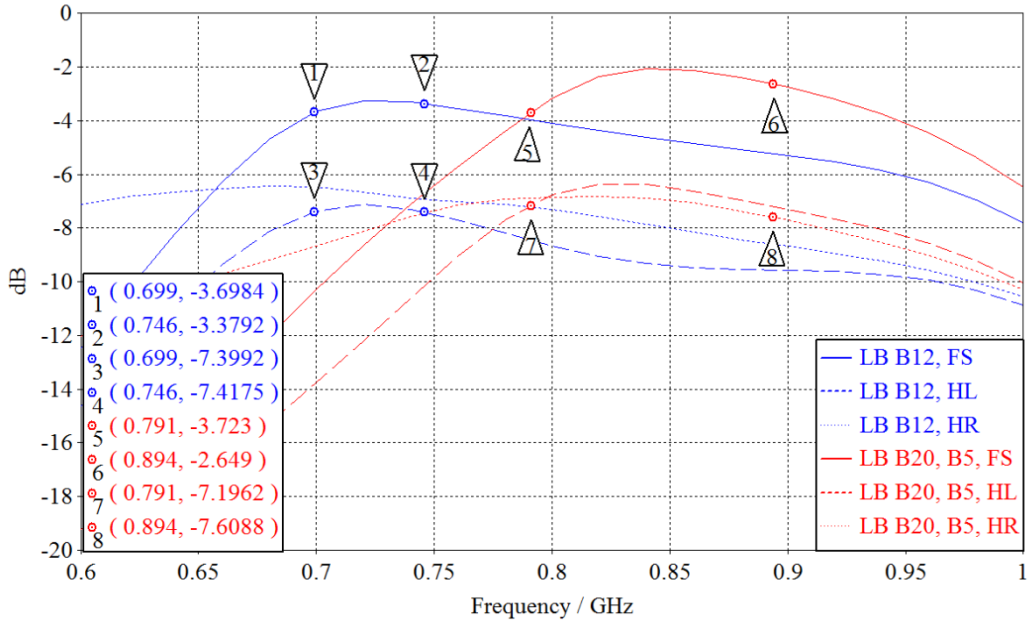

Figure 31. Total efficiency of design 1 LB main antenna in bands 12, 20 and 5 in the presence of hand.

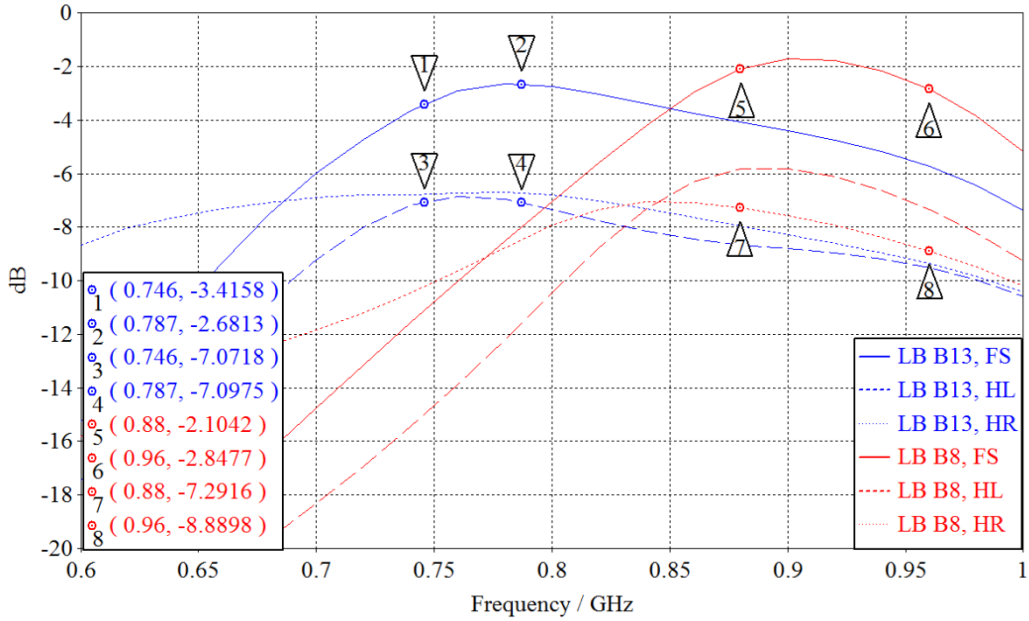

Figure 32. Total efficiency of design 1 LB main antenna in bands 13 and 8 in the presence of hand.

Similarly, simulation results for LB MIMO antenna are shown in Figure 33. It is shown that LB MIMO antenna total efficiency is degraded approximately 2 dB by both hand grips.

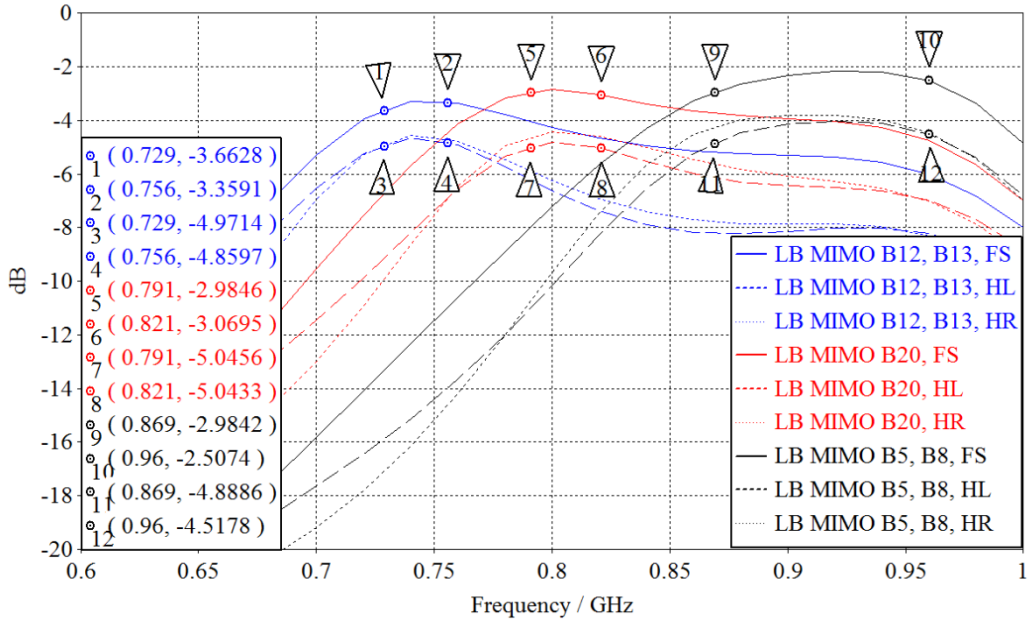

Figure 33. Total efficiency of design 1 LB MIMO antenna in the presence of hand with different tuner settings.

MB and HB main antenna total efficiency in the presence of hand is illustrated in Figure 34. Significant degradation in MB performance is observed with left hand grip which causes attenuation of 9 dB comparing to free space results. Right hand grip degrades the performance by 3 dB. HB performance is worse in the right hand which causes approximately 6 dB loss. Left hand degrades total efficiency by about 3 dB.

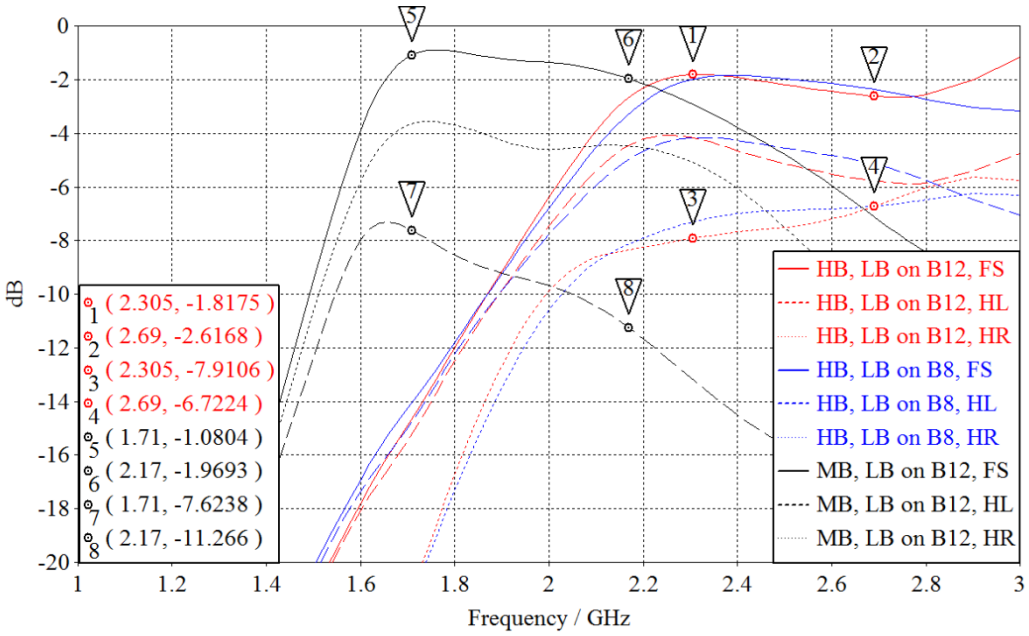

Figure 34. Total efficiencies of design 1 MB and HB main antennas in the presence of hand with different LB tuner settings.

MB and HB MIMO antenna total efficiency in the presence of hand is presented in Figure 35. Again MIMO antenna total efficiency suffers only a little due to hand grip. Observed degradation is at most 2 dB in MB and HB MIMO antennas.

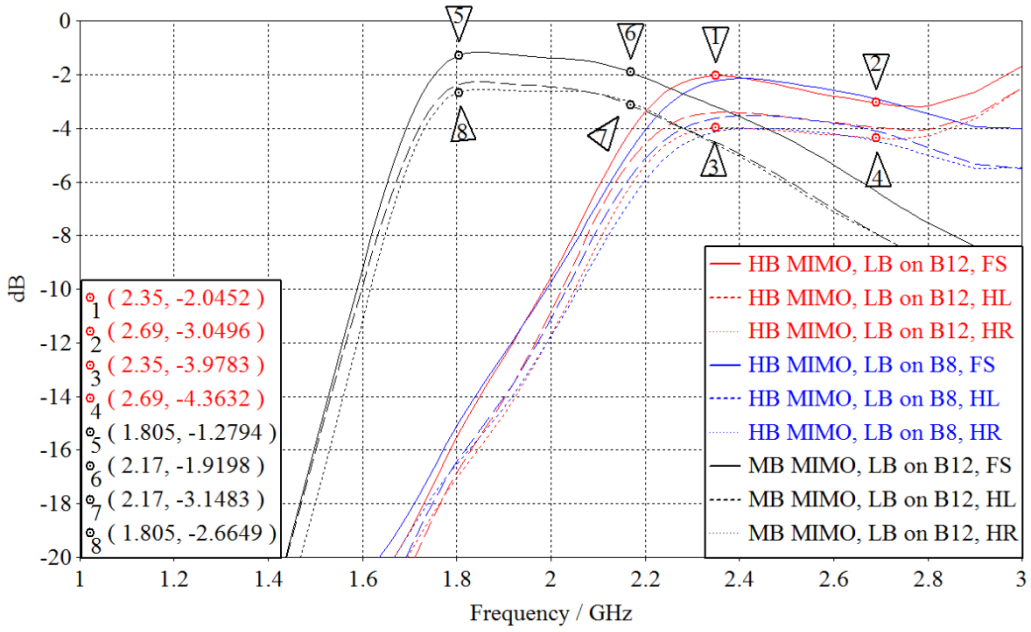

Figure 35. Total efficiencies of Design 1 MB and HB MIMO antennas in the presence of hand.

As shown in free space simulations earlier, ECC results were near the specified limit of 0.5 in LB where the worst case result 0.46 occurs when tuned to band 12. Band 12 ECC performance was verified in the presence of both hand grips. Worst case graphs from band 12 are shown in Figure 36. Hand grip reduces the correlation to 0.3 in right hand and in left hand to as low as 0.06.

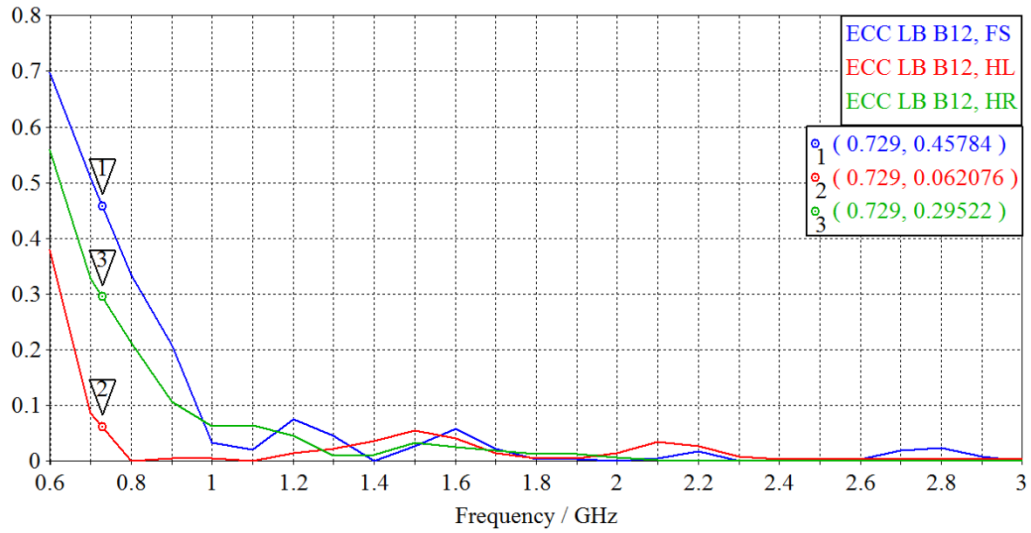

Figure 36. Design 1 band 12 ECC performance in the presence of hand.

7.3. Results of the design 2 in free space (FS)

Matching of the main antennas with both tuner positions of the LBHB antenna is shown in Figure 37. It can be seen that with tuning inductor value 13.2 nH all bands requiring CA operation can be covered with the matching better than -5.7 dB. The other tuner setting is only for band 8 while it also improves band 7 performance while band 30 is detuned. MB antenna performance is almost unaffected by tuner as antennas are well isolated, so only a single MB matching graph is shown.

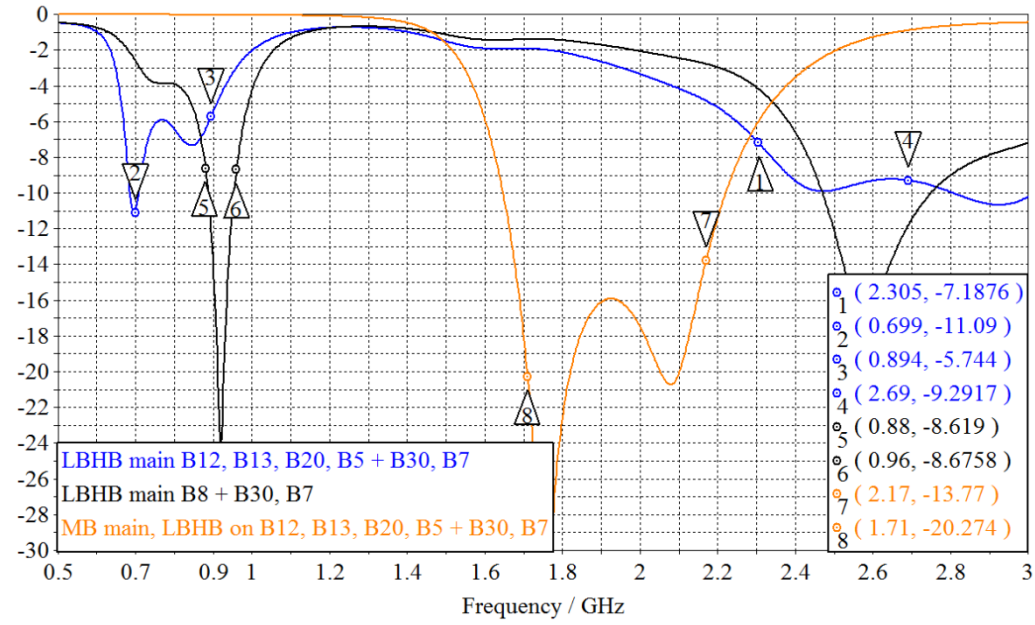

Figure 37. Design 2 main antenna matching with different tuner settings.

MIMO antenna matching results are given in Figure 38. First tuner setting is used to cover bands 12, 13 and 20 from LB to go with bands 30 and 7 in HB. Second setting covers bands 5 and 8 from LB with bands 30 and 7 from high band. All simulated matching results are better than -5.5 dB which meets the requirements. It can also be seen that HB MIMO matching performance does not suffer much from LBHB tuning like in main antenna. MB MIMO antenna matching is shown to be excellent and independent from the LBHB element tuning.

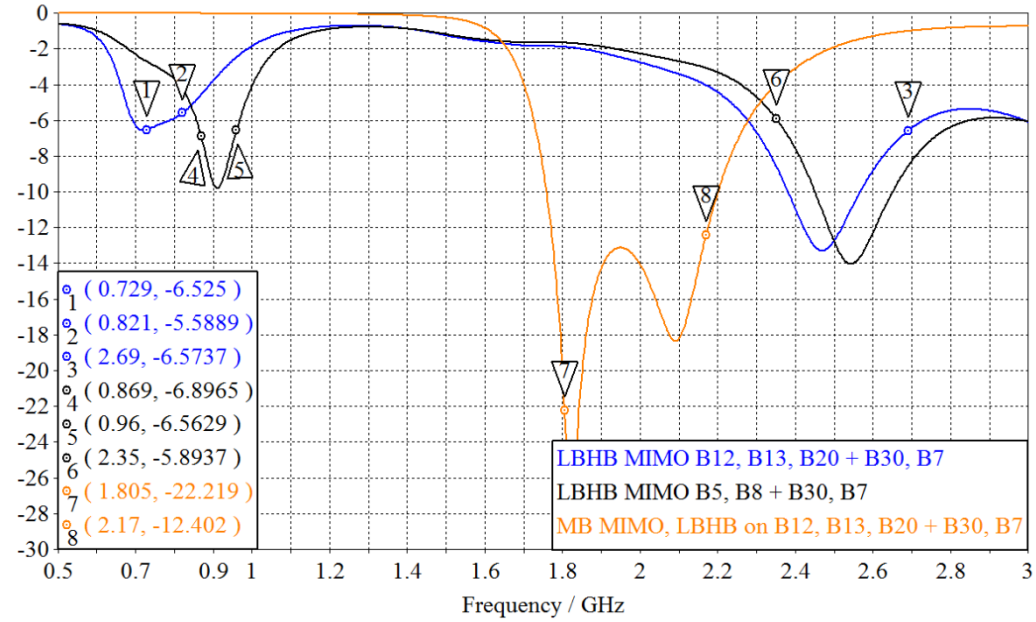

Figure 38. Design 2 MIMO antenna matching with different tuner settings.

Total efficiencies of the main antennas are illustrated in Figure 39. Results are better than -4 dB on LB and better than -2.2 dB in HB while MB results are excellent, better than -1.6 dB.

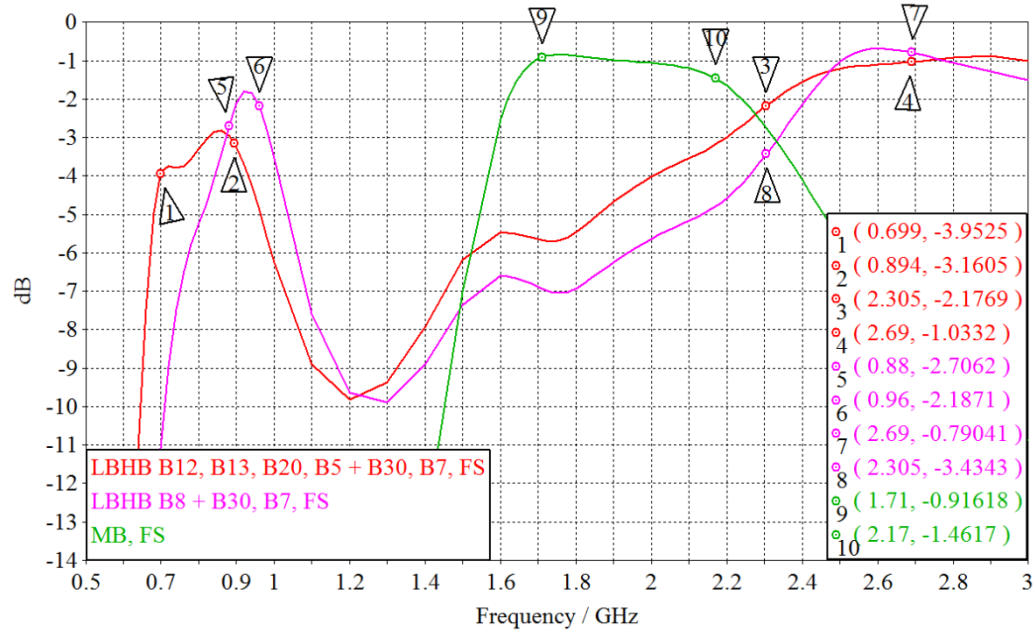

Figure 39. Design 2 main antenna total efficiency with different tuner settings.

LBHB MIMO antenna has slightly worse performance in efficiency compared to main antenna which is shown in Figure 40. Results in LB are at worst a bit better

than -5 dB and in HB better than -2.4 dB. Additionally it is shown that MB efficiency is almost identical in main and MIMO antennas.

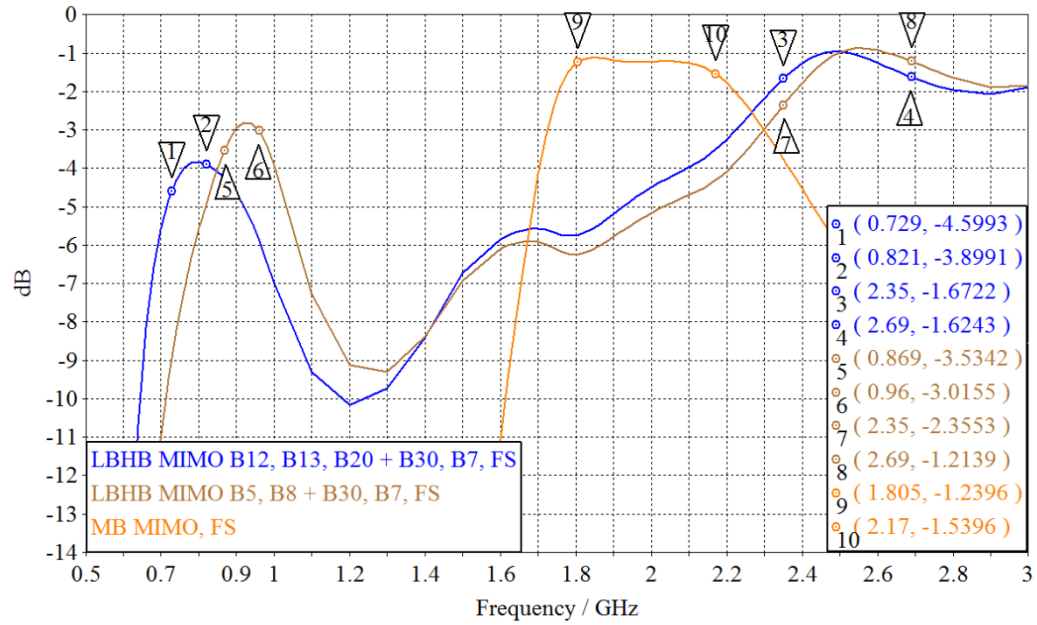

Figure 40. Design 2 MIMO antenna total efficiency with different tuner settings.

In Figure 41 is visualization of the ECC performance between main and MIMO antennas. Due to LBHB antenna feed location being away from the corners of the device LB ECC is around 0.6 which does not meet the specification. However, it is expected that the correlation would be reduced if more complex realistic phone model was used in simulations. MB and HB results are well below requirements. Multiplexing efficiency shown in Figure 42 is at worst -6.1 dB at band 12. When comparing this to the -4.5 dB achieved with separate antenna elements there is a slight decrease in MIMO performance at LB.

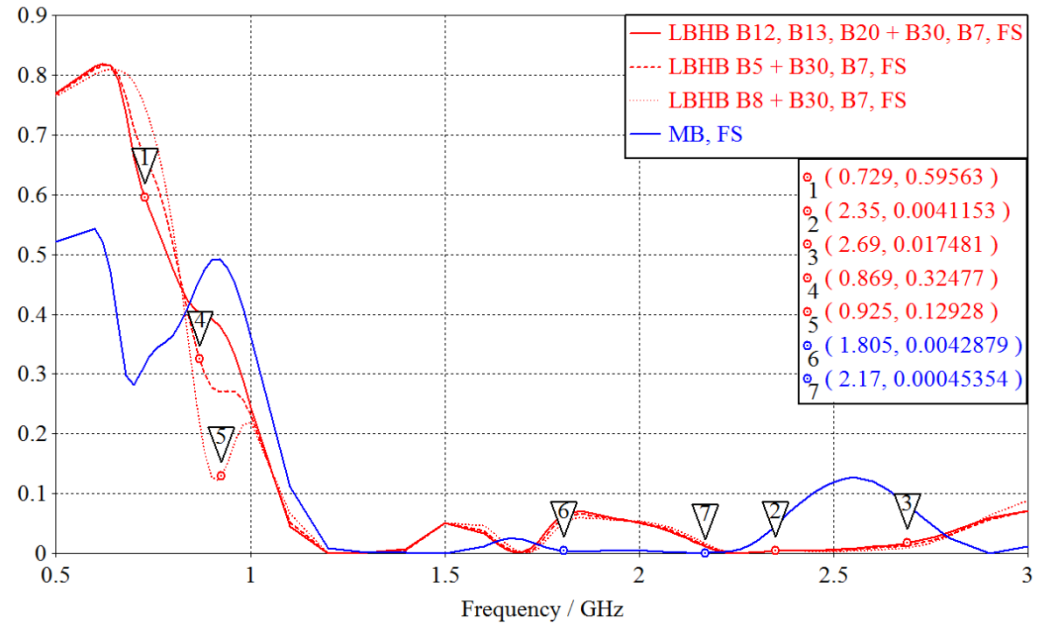

Figure 41. Design 2 ECC results.

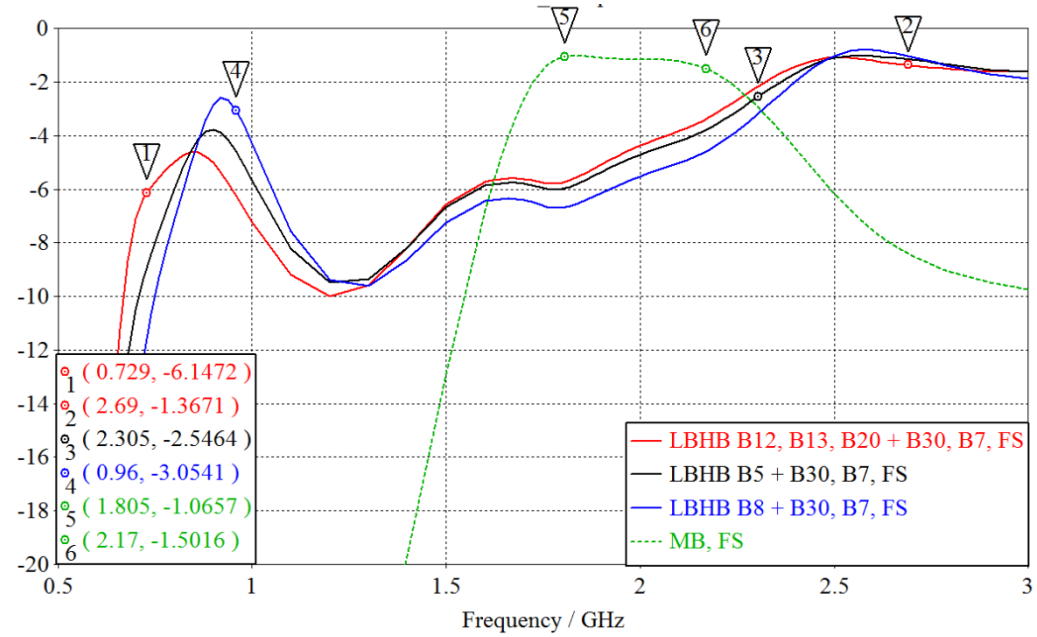

Figure 42. Design 2 multiplexing efficiencies with different tuner settings.

7.4. Results of the design 2 in left and right hand grips (HL and HR)

Results of simulations in the presence of hand are presented next. Figures are again showing the comparison between free space, left and right hand grip simulations.

Markers in figures denote the edges of the required frequency bands. Band specific results are shown later in section 7.5.

In Figure 43 and Figure 44 matching results of main antennas are presented using both tuner positions. When LB is tuned to cover bands 12, 13, 20 and 5, it can be seen from Figure 43 that on the right hand grip matching of the highest band 5 is degraded to -4.7 dB. This is however still acceptable as is the similar result of -4.2 dB in band 8 in Figure 44 caused by left hand grip. Both worst case results in LB are caused by slight detuning towards lower frequencies due to hand grip. MB matching performance is acceptable in all cases despite the slight detuning towards lower frequencies in right hand grip. HB results are great in free space and with right hand grip but performance is degraded in case of left hand grip. However, matching of -4.7 dB achieved is still acceptable. It is to be noted that band 30 is not needed simultaneously with band 8 so the worst case results in Figure 44 can be omitted and results taken from CA case in Figure 43.

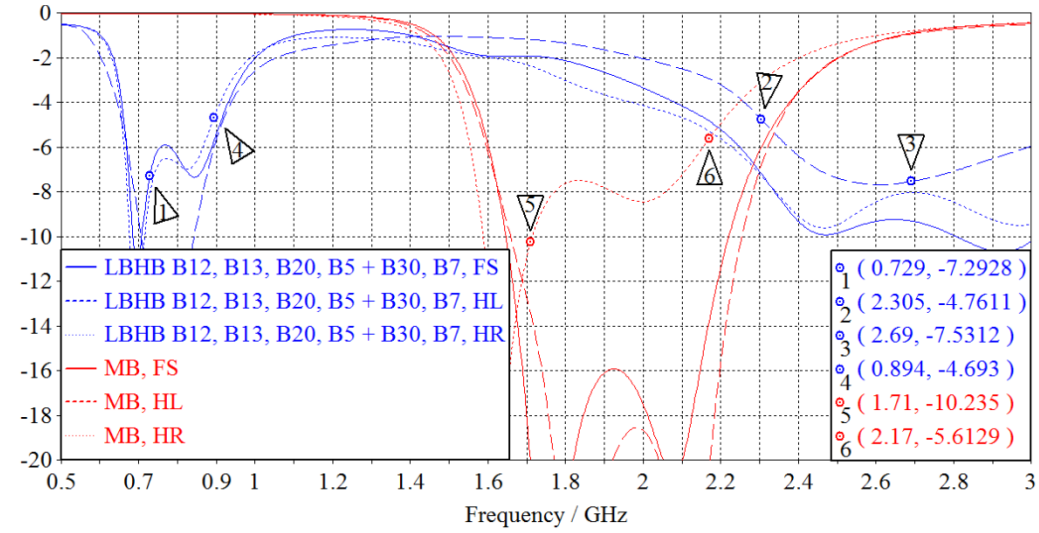

Figure 43. Design 2 matching of main antennas in the presence of hand with LB tuned to bands 12, 13, 20 and 5.

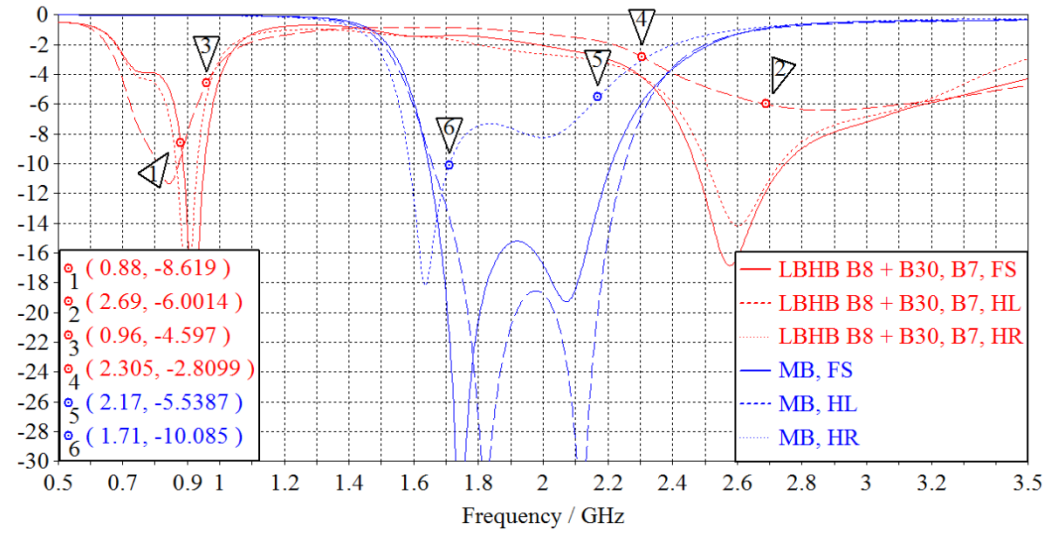

Figure 44. Design 2 matching of main antennas in the presence of hand with LB tuned to band 8.

Matching results of MIMO antennas are presented in Figure 45 when LB is tuned to bands 12, 13 and 20. Right hand grip causes severe detuning in band 20 where results are at worst only -3.9 dB. Even though this result is worse than targeted 4 dB, it is considered acceptable as the matching on band 20 could be improved by using additional tuning inductor which has inductance value between inductances used in simulated proposal. Other bands and hand grips have sufficient performance. Results shown in Figure 46 are from the situation when LB is tuned to bands 5 and 8. It is shown that all bands have matching better than -5 dB in this case.

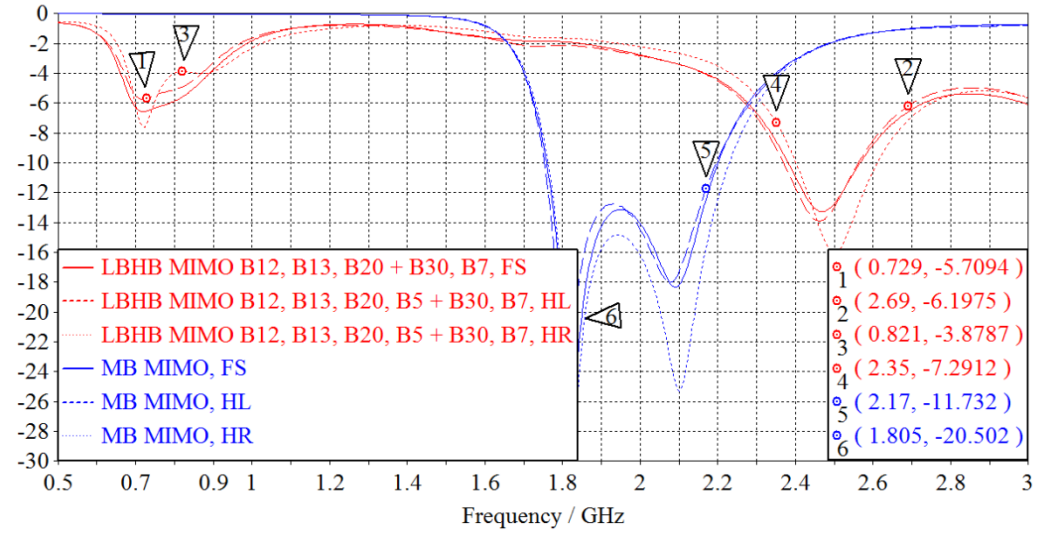

Figure 45. Design 2 matching of MIMO antennas in the presence of hand with LB tuned to bands 12, 13, and 20.

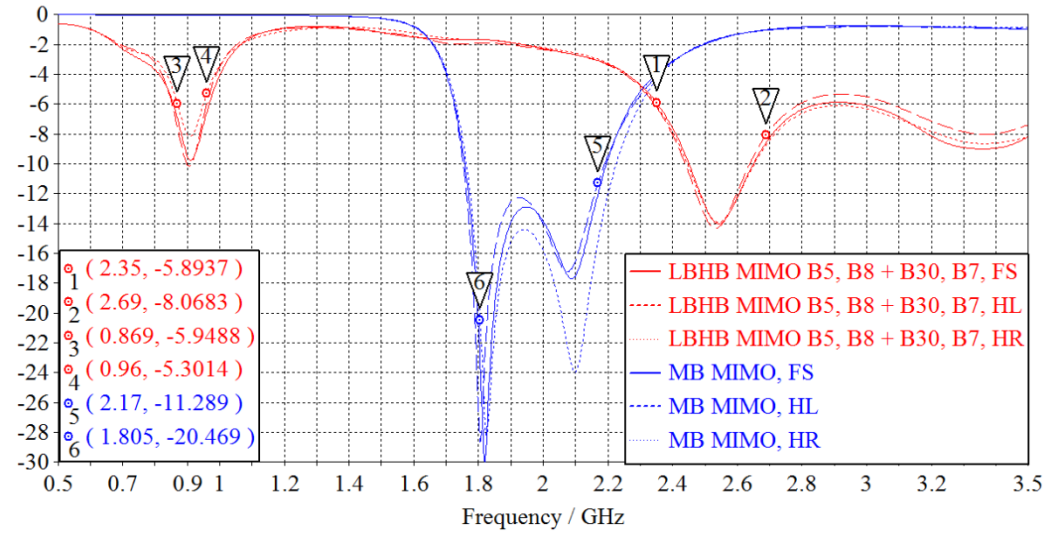

Figure 46. Design 2 matching of MIMO antennas in the presence of hand with LB tuned to bands 5 and 8.

Total efficiencies of main antennas in the presence of hand compared to free space are shown in Figure 47 and Figure 48, with a single LB tuner setting in each. Results show that a typical attenuation caused by hand is 4 – 6 dB at LB frequencies while differences between left and right hand grip is rather small. Situation is different in MB and HB frequencies where the attenuation difference between hands is almost 8 dB. Worst simulated total efficiency was on band 1 receiver frequencies around 2.1 GHz where results are -11.3 dB at worst.

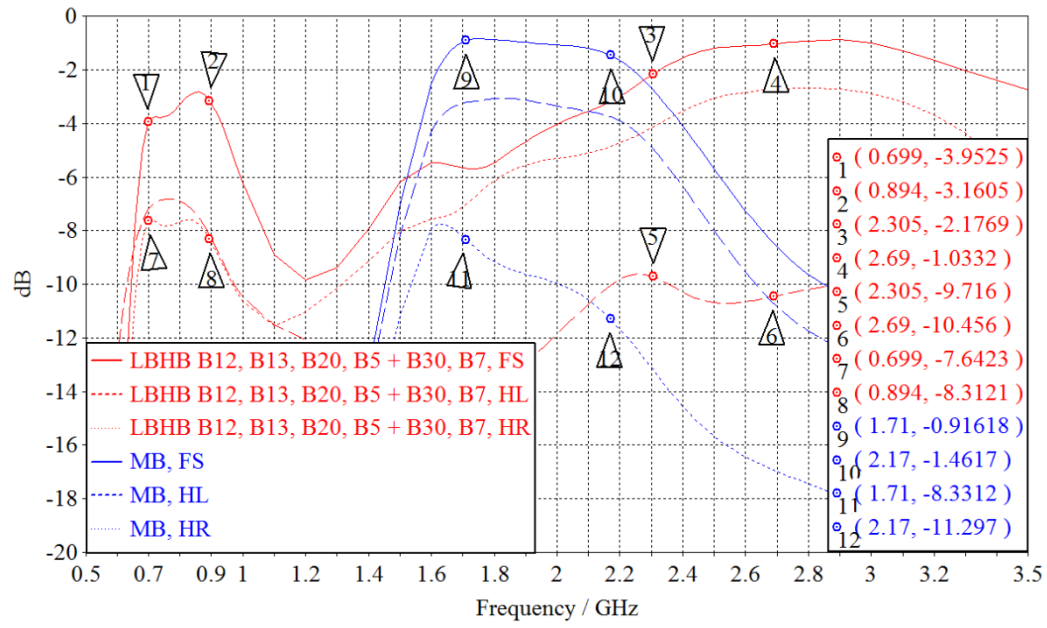

Figure 47. Design 2 main antenna total efficiencies in the presence of hand with LB tuned to bands 12, 13, 20, 5, 30 and 7.

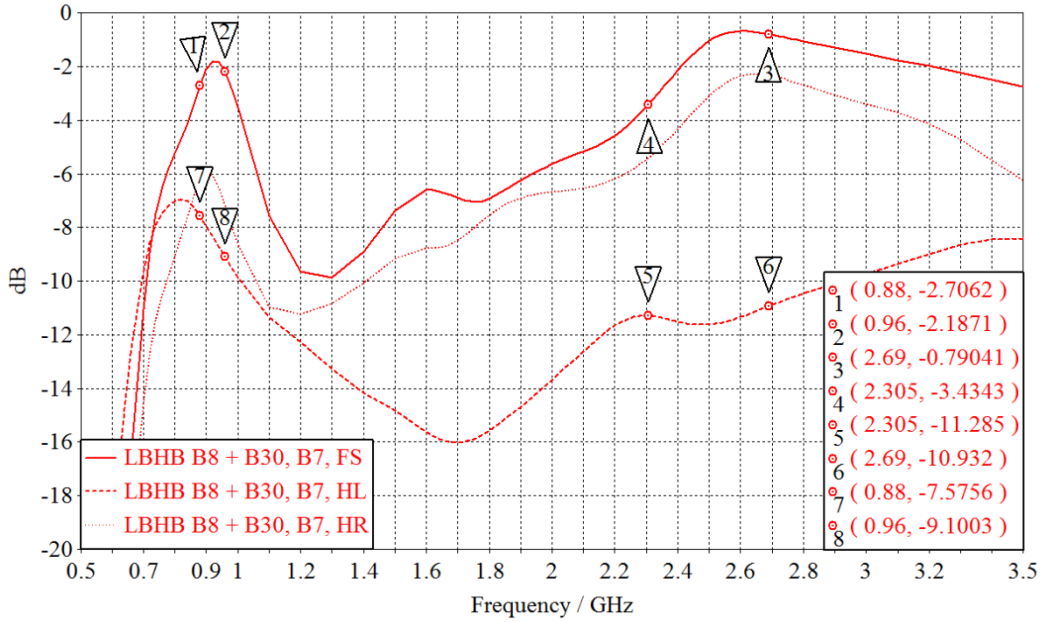

Figure 48. Design 2 main LBHB antenna total efficiency in the presence of hand with LB tuned to band 8.

The effect of hand grip in MIMO antenna total efficiency is illustrated in Figure 49 and Figure 50 both figures covering a single LB tuner state. Both figures indicate that total efficiency degrades 2 – 3 dB in LB frequencies due to both hand grips. MB and HB suffer approximately 1 – 2 dB degradation due to hand grips.

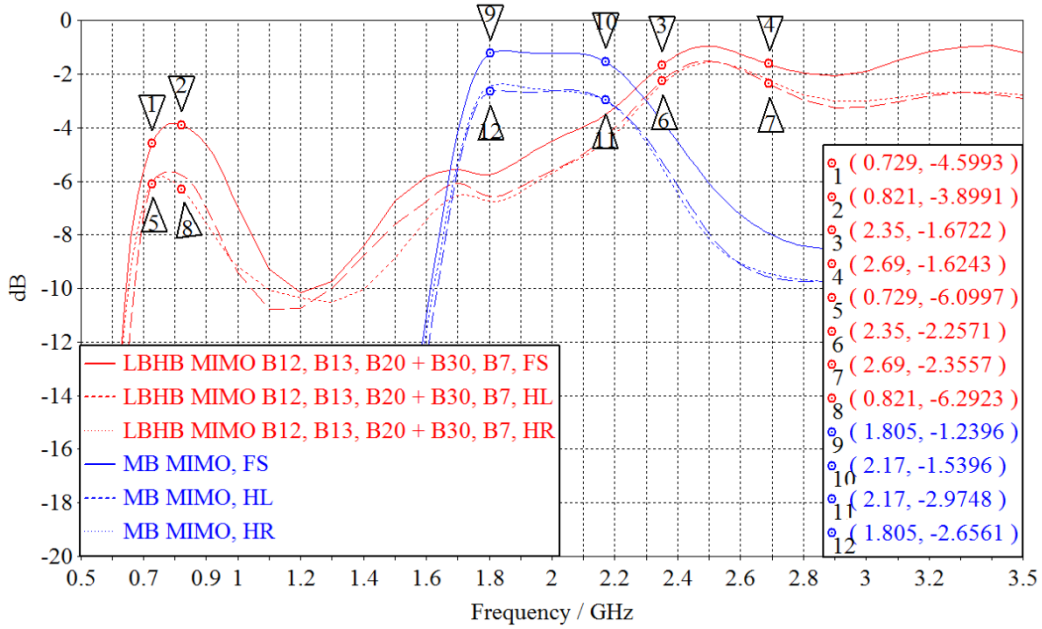

Figure 49. Design 2 MIMO LBHB antenna total efficiency in the presence of hand with LB tuned to bands 12, 13 and 20.

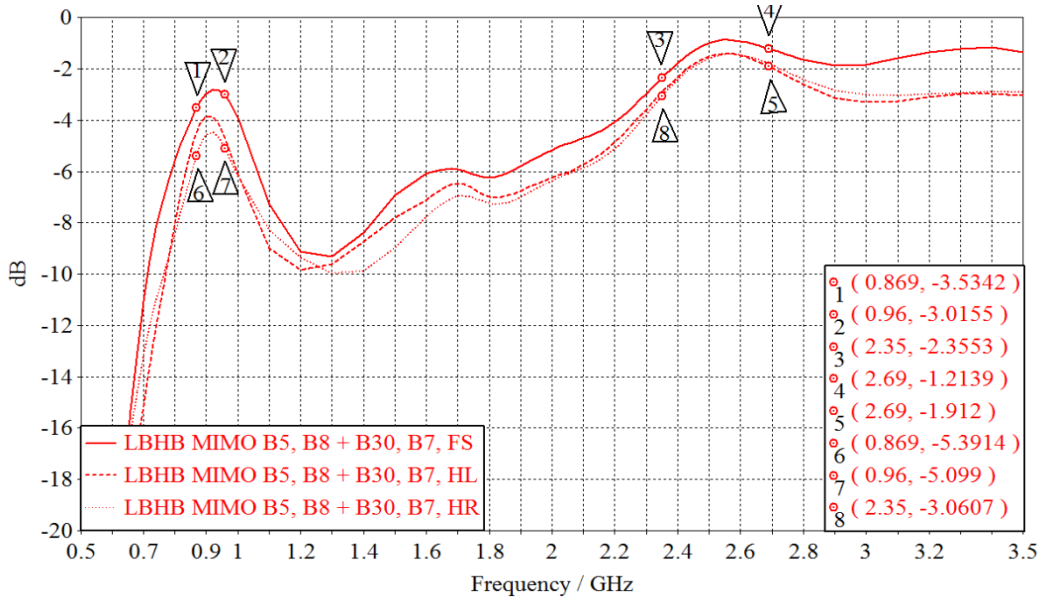

Figure 50. Design 2 MIMO antenna total efficiency in the presence of hand with LB tuned to bands 5 and 8.

In free space simulations LB ECC results failed to meet the specified limit of 0.5. Simulation results with hand grip shown in Figure 51 illustrate the improved ECC in the presence of hand. Correlation results improve from 0.60 in free space to 0.39 and 0.17 in left and right hand grips, respectively. Results show the performance on the lowest frequency band 12 which has worst performance.

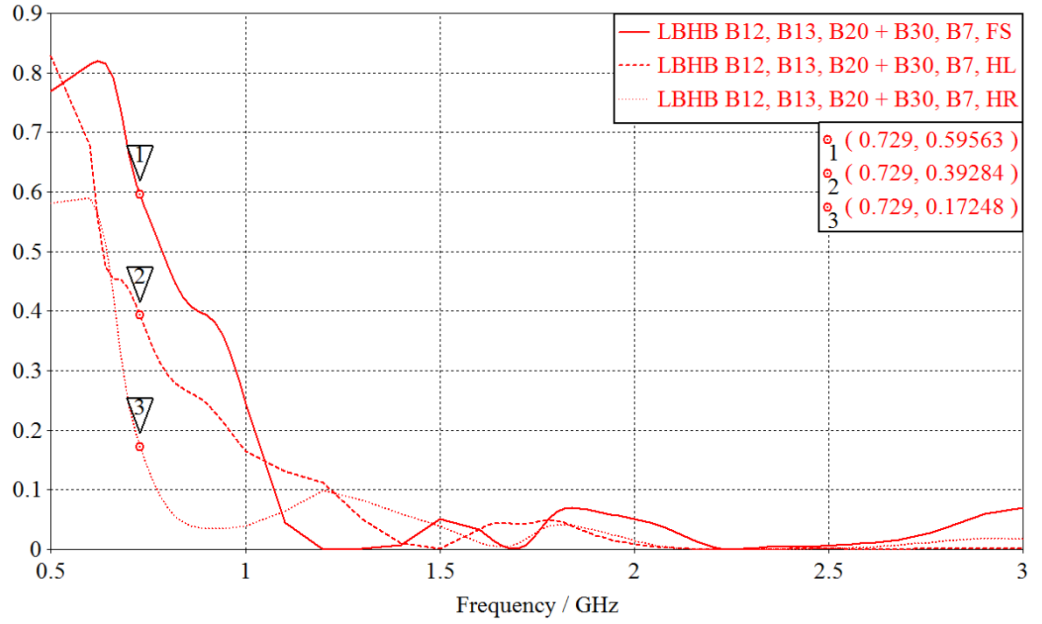

Figure 51. Design 2 LB ECC performance in the presence of hand.

7.5. Key simulation results

The most important simulation results of the design 1 and design 2 are gathered in Table 7 and Table 8, respectively. Worst case results for each frequency band are shown. Total efficiency result with hand grip is the result from worse side.

Table 7. Gathered results of the design 1

	Total efficiency FS [dB]	Total efficiency with hand grip [dB]	Matching FS [dB]	ECC FS	Multiplexing efficiency FS [dB]
B12 main	-3.7	-7.4	-6.7	0.38	-4.5
B12 MIMO	-3.7	-5.0	-9.6		
B13 main	-3.4	-7.1	-8.3	0.35	-4.2
B13 MIMO	-3.4	-4.9	-8.1		
B20 main	-3.7	-7.2	-6.7	0.26	-4.0
B20 MIMO	-3.1	-5.0	-7.7		
B5 main	-3.0	-7.6	-6.0	0.11	-2.9
B5 MIMO	-2.7	-4.9	-9.5		
B8 main	-2.1	-8.9	-6.9	0.05	-2.8
B8 MIMO	-2.5	-4.5	-9.3		
B4 main	-1.8	-11.1	-10.2	0.0	-1.9
B4 MIMO	-1.8	-2.9	-10.9		
B3 main	-1.1	-9.1	-10.5	0.0	-1.1
B3 MIMO	-1.3	-2.7	-12.6		
B2 main	-1.3	-9.6	-10.2	0.0	-1.3
B2 MIMO	-1.3	-2.6	-10.4		
B1 main	-2.0	-11.3	-9.6	0.0	-1.9
B1 MIMO	-1.9	-3.1	-10.4		
B30 main	-2.0	-7.9	-10.1	0.0	-1.9
B30 MIMO	-2.2	-4.0	-10.3		
B7 main	-2.6	-7.5	-5.7	0.02	-2.9
B7 MIMO	-3.0	-4.4	-5.3		

Table 8. Gathered results of the design 2

	Total efficiency FS [dB]	Total efficiency with hand grip [dB]	Matching FS [dB]	ECC FS	Multiplexing efficiency FS [dB]
B12 main	-3.9	-7.8	-6.3	0.60	-6.1
B12 MIMO	-4.6	-6.1	-6.4		
B13 main	-3.8	-7.8	-5.9	0.57	-5.8
B13 MIMO	-4.2	-5.9	-6.3		
B20 main	-3.4	-7.8	-6.2	0.49	-5.1
B20 MIMO	-3.8	-6.3	-5.6		
B5 main	-3.2	-8.3	-5.7	0.32	-4.0
B5 MIMO	-3.5	-5.4	-6.9		
B8 main	-2.7	-9.1	-8.6	0.13	-3.1
B8 MIMO	-3.0	-5.1	-6.6		
B4 main	-1.4	-11.1	-15.1	0.00	-1.4
B4 MIMO	-1.4	-2.9	-13.2		
B3 main	-1.0	-9.6	-16.5	0.00	-1.1
B3 MIMO	-1.2	-2.7	-23.3		
B2 main	-1.1	-9.9	-15.9	0.00	-1.2
B2 MIMO	-1.2	-2.7	-12.9		
B1 main	-1.5	-11.3	-13.8	0.00	-1.5
B1 MIMO	-1.5	-3.0	-11.9		
B30 main	-2.2	-10.0	-7.2	0.00	-2.5
B30 MIMO	-2.4	-2.3	-5.9		
B7 main	-1.2	-10.7	-9.2	0.02	-1.4
B7 MIMO	-1.6	-2.4	-6.6		

8. DISCUSSION OF RESULTS

In this chapter the performance of both designs is compared within the scope of this thesis. Both designs meet the specified requirements set for matching, total efficiency and envelope correlation coefficient as shown in the previous chapter. Comparable key figures discussed here are total efficiency including different RF front ends and respective antenna elements, total volume occupied by antennas and also the performance in the presence of hand grips. In addition, discussion about feasibility of designs is presented.

8.1. Performance comparison

When RF front end and total efficiencies of antennas are combined, results shown in Table 9 are obtained. Total efficiency comparison is done between design 1 with two different front end configurations and design 2 with a single front end configuration. Total efficiencies of each 3GPP band are taken from the worst case situations in free space. These worst case results are averaged to give a single worst case efficiency value for LB, MB and HB each. It can be seen that all proposals have FS total efficiencies within 1.1 dB window through all bands despite different front end and antenna configurations. Improved antenna efficiency of the design 2 comparing to design 1 is a direct result of the increased volume. Design 1 with a four cable front end has a total of 0.8 dB worse total efficiency due to two diplexers in LB and MB than with the six cable front end. MB antenna performance of the design 2 is improved from design 1 due to bigger distance and thus better isolation between MB and HB antenna elements which reduces the mutual coupling and consequently increases the efficiency. Additionally, worst case results from both left (HL) and right hand (HR) grips are shown for LB, MB and HB.

Both designs have similar LB and MB performance when the user hand is present. Results of designs shown in are almost identical when HL results of design 1 are compared to HR results of design 2 and vice versa. Similarity of results was expected as the MB antenna is identical in both designs. On the other hand, despite differences in LB element size and feeding, chassis is the main radiator in LB and thus radiation properties were expected to be quite similar. Correspondence of HR and HL results of different designs is due to antennas positioned in opposite corners. The mirrored positioning can be seen from Figure 9 and Figure 14. Results show that LB and especially MB performance is strongly depending on which hand holds the device. When corner of phone including antenna is on the palm of hand near the thumb, efficiency degradation is obviously much more severe than in case of opposite hand grip where antenna is located near the edge of the palm. Because hand loads the coupling element when antenna is concealed by palm, it detunes antenna slightly. In this case hand also covers the area where electric field is strongest and thus absorbs more power which is shown as degraded total efficiency.

Table 9. Comparison of total efficiencies including antennas and RF front ends

Design 1 with 6 transmission lines	LB main	MB main	HB main	LB MIMO	MB MIMO	HB MIMO
Losses from duplexer [dB]	-2	-2	-2	-2	-2	-2
Losses from diplexer [dB]	0	0	0	0	0	0
Losses from switch [dB]	-0.2	-0.2	-0.2	-0.2	-0.2	-0.2
Total efficiency of a matched antenna, worst case average (FS) [dB]	-3.2	-1.6	-2.3	-3.1	-1.6	-2.6
Total efficiency of a matched antenna, worst case (HL) [dB]	-7.4	-11.3	-6.7	-5.0	-3.1	-4.0
Total efficiency of a matched antenna, worst case (HR) [dB]	-8.9	-4.6	-7.9	-5.0	-3.1	-4.4
Total efficiency of antenna and front end (FS) [dB]	**-5.4**	**-3.8**	**-4.5**	**-5.3**	**-3.8**	**-4.8**
Design 1 with 4 transmission lines and 2 diplexers	LB main	MB main	HB main	LB MIMO	MB MIMO	HB MIMO
Losses from duplexer [dB]	-2	-2	-2	-2	-2	-2
Losses from diplexers [dB]	-0.8	-0.8	0	-0.8	-0.8	0
Losses from switch [dB]	-0.2	-0.2	-0.2	-0.2	-0.2	-0.2
Total efficiency of a matched antenna, worst case (FS) [dB]	-3.2	-1.6	-2.3	-3.1	-1.6	-2.6
Total efficiency of antenna and front end (FS) [dB]	**-6.2**	**-4.6**	**-4.5**	**-6.1**	**-4.6**	**-4.8**
Design 2	LB main	MB main	HB main	LB MIMO	MB MIMO	HB MIMO
Losses from duplexer [dB]	-2	-2	-2	-2	-2	-2
Losses from diplexer [dB]	-0.4	0	-0.4	-0.4	0	-0.4
Losses from switch [dB]	-0.2	-0.2	-0.2	-0.2	-0.2	-0.2
Total efficiency of a matched antenna, worst case average (FS) [dB]	-3.4	-1.3	-1.7	-3.8	-1.3	-2.0
Total efficiency of a matched antenna, worst case (HL) [dB]	-9.1	-3.8	-11.3	-6.1	-3.0	-2.4
Total efficiency of a matched antenna, worst case (HR) [dB]	-7.9	-11.3	-4.1	-8.6	-3.0	-2.4
Total efficiency of antenna and front end (FS) [dB]	**-6.0**	**-3.5**	**-4.3**	**-6.4**	**-3.5**	**-4.6**

It can be arguably said that achieved MB free space efficiency is even too good. A little degradation in performance could possibly either make the element even smaller or it could be moved away from the hand grip towards the center of the device.

The biggest difference between designs comes from the HB performance as the designs are completely different in that sense. Despite very small distance between LB and HB antennas in design 1, free space total efficiencies of both antennas are

quite good. Both elements have matching circuits with band pass responses which improve the isolation between the antennas and enable good performance. Distance between MB and HB elements is much bigger to ensure sufficient isolation between antennas with small separation in operating frequency. Also MB antenna matching circuit has band pass responses to enhance isolation. Slight degradation in total efficiencies can be observed at the high MB frequencies and low HB frequencies at bands 1 and 30 due to mutual coupling. HB results do not vary much between hand grips in design 1 as the HB antenna is near the center of the bottom edge of phone which is rather close to same position regarding the palm in both hand grip cases.

Design 2 HB performance is better in free space but left hand grip leads to trouble in main antenna total efficiency. This is due to same phenomenon explained earlier that causes MB performance to drop in one hand grip. In both designs, MIMO antenna performance is affected only mildly by hand grip as MIMO antennas are located on top of the phone which is mostly out of the reach of hand grips. The effect of the user's head was not simulated in this thesis, but it is expected to affect MIMO antennas more than main antennas as they are located very close to the head in talk position.

8.2. Discussion on effect of antenna locations

Few observations on antenna locations were made based on the simulation results. LB frequencies are more robust to efficiency degradation due to hand grip which implies that LB antenna elements can be positioned to the corners of the device where effects of hand grip are most severe. Also, as the chassis wave mode is so dominant on low frequencies, LB results with both left and right hand grips are very close to each other. Another reason encouraging the positioning of LB antenna to the corner of the chassis is improving ECC. It was noted that when feeding point was moved from the corner (Design 1) to the 12 mm offset from the edge (Design 2), ECC performance was considerably reduced as the radiation patterns of main and MIMO antennas got more similarly shaped. Because ECC depends strongly on feed location of both LB elements, it restricts positioning of LB MIMO element quite a bit. If main LB antenna feed is in the left bottom corner, only practical positions for LB MIMO antenna feed are near the left top corner or near the right bottom corner. Otherwise sufficient ECC performance is difficult to achieve.

Hand grip caused more severe difficulties with antennas associated to MB and HB. Hand attenuates the high frequencies more than low ones. Also antenna element radiates more compared to chassis in high frequencies. These things together lead to bigger losses occurring in hand grip especially if antenna is located inside the corner of the device concealed by the user's palm. On the opposite hand grip however, attenuation was simulated to be much smaller if MB or HB antenna was located on the corner of the device. Based on the performance of HB antenna in design 1, it appears that ideal position for high frequency elements (MB and HB) would be near

the center of the bottom edge where effects of both hand grips are quite even. ECC did not cause any problems on MB and HB due to rather big distance comparing to wavelength between main and MIMO elements. This gives freedom in MB and HB MIMO element positioning.

Positioning all MIMO antennas on top of the device is good for efficiency performance in free space and hand grip positions. However, visual and thus space requirements may force the selection of other locations for MIMO antennas. Also, an extra attenuation caused by the user's head not simulated in this thesis drives a search for alternative MIMO antenna locations. Simulated results of multiplexing efficiency show that on MB and HB is achieved the best MIMO performance and along that the highest data rates with both solutions. This is direct consequence from the low ECC and high efficiency on those frequencies. On the other hand, LB MIMO performance suffers slightly from higher ECC and lower efficiency.

8.3. Comparison of antenna volume and design complexity

Total volumes occupied by antennas and antenna clearances are compared in Table 10. It can be seen that the design 1 has significantly smaller total volume. Due to need to match the same antenna element for both LB and HB simultaneously the volume of the required element is considerably bigger. For example, combined volume of LB and HB main antennas of the design 1 (1504.5 mm^3) is much smaller than the volume of the combined LBHB antenna in design 2 (1750 mm^3). In addition to enlarging the antenna also the antenna clearance was increased out of necessity. This leads to increase in volumes of the MB antennas, too, even though this was not necessary performance-wise. In both designs, LB performance was the limiting factor determining the antenna clearance. In design 1 smaller clearance was achieved as larger LB tuning range was allowed. In design 2 tuning range was reduced due to required simultaneous LB and HB resonances. If tunable matching component value was changed too much to tune LB, it detuned the HB resonance. Thus, bigger clearance was required to obtain larger bandwidth in LB. Because total efficiencies of the both antennas without front ends are almost equal, it is reasonable to compare the total volumes.

Table 10. Total volumes and antenna clearances of the proposals

Design 1	Volume [mm^3]	Clearance [mm]
LB Main	1402.5	8.5
LB MIMO	1320	8
MB Main	255	8.5
MB MIMO	240	8
HB Main	102	8.5
HB MIMO	96	8
TOTAL VOLUME	**3415.5**	
Design 2	Volume [mm^3]	Clearance [mm]
LBHB Main	1750	10
LBHB MIMO	1575	9
MB Main	300	10
MB MIMO	270	9
TOTAL VOLUME	**3895**	

When considering exclusively the total volumes of the antennas and not considering transmission lines etc., it is obvious that design with three separate antennas is more feasible as it achieves same performance with smaller total volume. This is very important in mobile devices where space is a scarce resource. Only drawback of the design 1 is that the bigger portion of the bottom and top end surface are covered by antennas which leave less space for other components like speakers, USB ports etc. typically located in those places.

Antennas are usually connected to RF front end by using transmission lines. Connection from front end to each antenna is required. In case of six separate antenna elements this would mean six transmission lines which would eat a lot of space inside the device. In section 6.2 it was shown that while using this design, space can be saved by using a diplexer at both ends of the single transmission line which allows one to be left out from both main and MIMO front ends. However, this would cause additional 0.8 dB loss from two diplexers to bands which are using the shared transmission line. As mentioned earlier, MB and HB cannot be separated with diplexers. Thus, MB and HB antennas must be connected to RF front end through different transmission line. Design 2, on the other hand, can be implemented directly with a total of four transmission lines with only a single diplexer in transmission lines connecting LBHB main and MIMO antennas to RF front end. The number of required transmission lines is also subject to change along with the location of RF front end. Space consuming transmission lines can be partially replaced if front end is located next to main or MIMO antennas. In this case some antennas can be fed via PCB to save space otherwise required to accommodate the transmission lines.

By using quadplexers on CA bands instead of duplexers it is possible to reduce the number of required transmission lines to one for both main and MIMO antennas. In this approach there are two big drawbacks. First, losses increase in all bands 0.8 dB as two diplexers are needed – one at both ends of the transmission lines. Additional losses occur on MB and HB CA bands due to required quadplexers which attenuate signal 0.5 dB more than regular duplexers. The second drawback comes from the fact that frequency bands and thus CA bands are different around the world. As different quadplexers are needed for all the MB and HB CA combinations, all country variants require different quadplexers combinations. This is much more expensive than approaches without quadplexers shown in this thesis as they are basically global variants covering most of the significant LTE bands.

Both designs shown in this thesis required tuners in LB matching circuit to cover all LB bands specified. Design 1 has more complex tuners as it requires SP4T and SP3T switches in main and MIMO antenna matching circuits, respectively. Design 2 can handle all bands with SP2T switches in both main and MIMO antennas despite covering also HB frequencies with same element. This is again possible due to bigger volume which directly leads to bigger bandwidths. Amount of tuning components is larger in design 1, as it requires a total of 29 matching components and two switches. Design two is matched with a total of 22 matching components and two switches. The space required by matching circuits is not included in volume comparison tables.

8.4. Conclusive discussion

Advantages of the design 1 are the following. It has a smaller antenna volume comparing to design 2. Despite smaller total volume with front end with six transmission lines design 1 achieves same total efficiency as design 2. Separate antenna elements are easier to design as no simultaneous resonances are needed on low and high frequencies. Performance difference between left and right hand grip is small in HB antenna. The biggest disadvantage of the design 1 is the number of needed space consuming transmission lines. Designer can either accept a total of six transmission lines or use two diplexers to reduce the number of transmission lines to four with a cost of decreased efficiency.

Design 2 offers same total efficiency with four transmission lines than design 1 using front end with six transmission lines. However, much larger antenna volume is the price to pay to achieve this. High ECC on LB is also a concern in design 2 due to the antenna feed positioning. HB performance is good in free space, but varies much between left and right hand grips.

Both designs are suitable for global operation with only minor hardware changes. Depending on used CA combinations in variants it is possible to use the designs globally without any changes in hardware. Only if two component carriers use the same antenna switch, quadplexers replacing duplexers are needed to support CA.

Common drawback of proposed antennas is MB antenna sensitivity to hand grip and uneven efficiency degradation of MB antenna between left and right hand grips.

Based on the results, it seems most feasible to use separate antenna elements with the front end solution reducing the number of transmission lines to four. This combines sufficient total efficiency, smaller antenna volume and fewest number of connections from the front end to the antennas.

9. CONCLUSIONS

To meet the increasing demand for higher data rates in mobile systems, carrier aggregation is one of the novel features introduced in LTE-Advanced. Multiple carriers from different frequency bands can be aggregated to increase the total bandwidth of a single user. In this thesis has been designed and simulated two different mobile antenna solutions suitable for three band downlink carrier aggregation. Total efficiency of solutions including antennas and suitable RF front end is compared along with the total volume occupied by the antennas.

The first proposed design has separate antenna elements for low, mid and high bands with MIMO antennas. Two different front end configurations are proposed for this design. Front end with separate transmission lines to all antennas has higher total efficiency but transmission lines consume a lot of space. Thus, more feasible front end solution with four transmission lines is proposed. The drawback of this front end is increased losses due to additional diplexers.

The second proposed antenna solution has combined LB and HB element with separate MB elements, a total of four antennas including two MIMO antennas. MB elements are identical in both designs.

Simulated total efficiencies of the proposed designs are quite close to each other. The difference of the designs comes from the space requirements. To meet the set requirements in matching, total efficiency and MIMO performance, design 2 requires bigger antenna clearance and thus the total antenna volume is almost 500 mm^3 bigger. Design 1 is more compact, especially with the front end solution with four transmission lines.

Performance of the designs was also verified in both left and right hand grips. In both designs, performance degradation due to hand grip was noted to be significant in MB frequencies if MB antenna element was concealed by the user's palm. Design 2 experienced similar phenomenon in the HB, as well. Design 1 HB element was located in the middle of the device, so it was equally robust against both hand grips.

Based on the results acquired in this thesis, conclusion is that the solution with separate antenna elements is the more feasible for mobile devices. In this solution, an equal total efficiency can be achieved with significantly smaller total volume than in the design with combined LB and HB elements even after adding the losses of two diplexers to front end to reduce the number of coaxial cables.

10. REFERENCES

[1] Graf R. (1999) Modern Dictionary of Electronics. Newnes, 873 p.

[2] Vainikainen P., Holopainen J., Icheln C., Kivekäs O., Kyrö M., Mustonen M., Ranvier S., Valkonen R., and Villanen J.(2010) More Than 20 Antenna Elements in Future Mobile Phones, Threat or Opportunity? In. Antennas and Propagation. 3rd European Conference on, March 23 – 27, Berlin, vol., no., pp. 2940 – 2943.

[3] Miron, D. (2006) Small Antenna Design. Newnes, 303 p.

[4] Holopainen J. (2011) Compact UHF-band Antennas for Mobile Terminals: Focus on Modelling, Implementation, and User Interaction. Doctoral Thesis. Aalto University, School of Electrical Engineering, Department of Radio Science and Engineering, Helsinki, Finland.

[5] Chen Z. (2007) Antennas for Portable Devices. John Wiley & Sons Ltd., 290p.

[6] Volakis J. (2007) Antenna Engineering Handbook 4th edition. McGraw – Hill.

[7] Balanis C. (2005) Antenna Theory, Analysis and Design. John Wiley & Sons Ltd., 1050 p.

[8] Rahola J. (2009) Estimating the Performance of Matching Circuits for Antennas. In. Proceedings of the Fourth European Conference on Antennas and Propagation (EuCAP), pp. 1 – 3.

[9] Rahola J. (2008) Power waves and Conjugate Matching. IEEE Transactions on Circuits and Systems – II: Express Briefs, Vol. 55, No. 1, pp. 92 – 96.

[10] Zhang S. (2013) Investigating and Enhancing the Performance of Multiple Antenna Systems in Compact MIMO/Diversity Terminals. Doctoral Thesis. KTH Royal Institute of Technology, School of Electrical Engineering, Stockholm, Sweden.

[11] Stjernman A.(2006) Antenna Mutual Coupling Effects on Correlation, Efficiency and Shannon Capacity. In. EuCAP 2006, First European Conference on Antennas and Propagation. November 6 – 10, Nice, France, p. 1 – 6.

[12] Bode H., (1945) Network Analysis and Feedback Amplifier Design, Van Nostrad, N.Y.

[13] Fano R., (1950) Theoretical Limitation on the Broad-Band Matching of Arbitrary Impedances. Journal of the Franklin Institute, Vol. 249, January 1950 pp. 57-83, and February 1950, pp. 139-154.

[14] Ollikainen J. and Vainikainen P. (2002) Design and Bandwidth Optimization of dual-resonant antennas (ISBN 951-22-5891-9). Espoo, Finland, 41 p.

[15] Vainikainen P., Ollikainen J., Kivekäs O. and Kelander I. (2002) Resonator Based Analysis of the Combination of Mobile Handset Antenna and Chassis. IEEE Transactions on Antennas and Propagation, Vol. 50, No. 10, pp. 1433 – 1444.

[16] Villanen J., Ollikainen J., Kivekäs O. and Vainikainen P. (2006) Coupling Element Based Mobile Terminal Antenna Structures. IEEE Transactions on Antennas and Propagation, Vol. 54, No. 7, pp. 2172 – 2153.

[17] 3G Americas (Accessed 2.12.2013) MIMO Transmission Schemes for LTE and HSPA Networks. URL: http://www.3gamericas.org/documents/Mimo_Transmission_Schemes_for_LTE_and_HSPA_Networks_June-2009.pdf

[18] Blanch S., Romeau J. and Corbella I. (2003) Exact representation of antenna system diversity performance from input parameter description. IEEE Electronics Letters, Vol. 39, No. 9, pp 705 – 707.

[19] Tian R., Lau B., and Ying Z. (2011) Multiplexing Efficiency of MIMO Antennas. IEEE Antennas and Wireless Propagation Letters, Vol. 10, pp 183 – 186.

[20] 3GPP (Accessed 16.01.2014) Carrier Aggregation Explained. URL: http://www.3gpp.org/Carrier-Aggregation-explained

[21] Yuan G., Zhang X., Wang W. and Yang Y. (2010) Carrier Aggregation for LTE-Advanced Mobile Communication Systems. IEEE Communications Magazine, Vol. 38, No. 2, pp. 88 – 93.

[22] Ikonen P., Ellä J., Schmidhammer E., Tikka P., Ramachandran P. and Annamaa P. (2012) Multi-feed RF Front-ends and Cellular Antennas for Next Generation Smartphones. URL: http://www.pulseelectronics.com/download/3755/indie_technical_article/pdf

[23] Ollikainen J. (2004) Design and Implementation of Wideband Mobile Communications Antennas. Doctoral Thesis. Helsinki University of Techology, Department of Electrical and Communications Engineering, Radio Laboratory, Helsinki.

[24] Manteuffel D., Bahr A., Heberling D. and Wolff I. (2001), Design considerations for integrated mobile phone antennas. In. Proc. 11 th International Conference on Antennas and Propagation (ICAP'01), April 17 – 20, Manchester, UK, vol. 1, no., p. 252-256.

[25] Martínez-Vázquez M. and Sánchez-Hernández D. (2000) Design of a compact dual-band antenna for mobile communications handsets. In. Proc. 30th European Microwave Conference (EuMC 2000), October 2 – 6, Paris, France, vol., no., p. 413-416

[26] Optenni Ltd. (Accessed 20.11.2013) Optenni Lab Features URL: http://www.optenni.com/optenni-lab

[27] Rahola J. (2009) Bandwidth potential and electromagnetic isolation:

tools for analysing the impedance behaviour of antenna systems. 3rd European Conference on Antennas and Propagation. March 23 – 27, Berlin, Germany.

[28] Vishay Intertechnology (Accessed 14.1.2014) Inductors 101. URL: http://www.newark.com/pdfs/techarticles/vishay/Inductors101.pdf

[29] CTIA (Accessed 28.1.2012) Test Plan for Wireless Device Over-the-Air Performance revision 3.2. URL: http://files.ctia.org/pdf/CTIA_OTA_Test_Plan_Rev_3.2.pdf